

Temporal Variation for Magmatic Chemistry of the Sakurajima Volcano and Aira Caldera Region, Southern Kyushu, Southwest Japan since 61 ka and Its Implications for the Evolution of Magma Chamber System

Masaki TAKAHASHI^{*}, Tadashi OTSUKA^{**}, Hisashi SAKO^{**}, Hiroshi KAWAMATA^{***},
Maya YASUI^{*}, Tatsuo KANAMARU^{*}, Mei OTSUKI^{****}, Tetsuo KOBAYASHI^{*****},
Kazuhiro ISHIHARA^{*****} and Daisuke MIKI^{*****}

(Received October 5, 2011; Accepted December 19, 2012)

The temporal variation of magmatic chemistry and the evolution of magma chamber system of the Sakurajima volcano and Aira caldera region since 61 ka are studied based on the whole-rock major element, incompatible trace element and rare earth element chemistry of the eruptive products. The magmas of the Sakurajima volcano and Aira caldera region since 61 ka consist of four groups: (1) basaltic to basaltic andesitic magma of the mantle origin, (2) rhyolitic to high silica rhyolitic magma of the crustal origin, (3) dacitic magma and (4) andesitic magma produced by magma mixing of the mafic magma of mantle origin and the crustal felsic magma. Around 61 to 60 ka, basaltic to basaltic andesitic, andesitic and rhyolitic magmas were active in the Aira caldera region, and the Shikine andesite and the Iwato pyroclastic flow deposit were erupted. After a dormant period of about twenty-four thousands of years, the rhyolitic magmatism resumed and the voluminous high silica rhyolitic magma erupted at 29 ka to form the large-scale Osumi pumice fall and Ito pyroclastic flow deposits. The felsic magma produced the Iwato pyroclastic flow deposit and the Osumi pumice fall and Ito pyroclastic flow deposits were similar in composition; the latter high silica rhyolite can be derived from the former rhyolite by crystallization differentiation. The rhyolitic to high silica rhyolitic magma chamber system was stable and long-lived with duration of about thirty thousands of years. The magmatic activity of the Sakurajima volcano began at 26 ka after a quiescent period of about three thousands of years. The Moeshima rhyolitic magma discharged at 13.8 ka in the Aira caldera constitute another magma chamber system different from that of the Sakurajima volcano. The magma chamber system of the Sakurajima volcano was composed of the low Ti-P type and high Ti-P type dacitic and andesitic magmas. The magma chamber system of the low Ti-P type, which was active from about 14 to 4 ka, comprises at least the three sub-systems based on the whole-rock chemistry, while that of the historical eruption since 8th C is restricted to the high Ti-P type and consists of the three sub-systems, the youngest of which has been active since the subaqueous An-ei eruption at 1779AD. The duration of the activity of each magma chamber sub-system of the Sakurajima volcano is rather short, the time span of which is thousands to several hundreds of years.

Key words: Sakurajima volcano, Aira caldera, felsic magma, magmatic chemistry, magma chamber

1. Introduction

The Sakurajima volcano in southern Kyushu is one of the representative active dacitic to andesitic volcanoes in the late Quaternary Japanese islands, which is constructed on the southern margin of the large-scale Aira caldera with

a dimension of 24 × 20 km. The eruption of the Sakurajima volcano is now continuing from the Showa crater at the upper slope of the eastern flank of the volcano. The magma of the Sakurajima volcano is estimated to be being fed from the magma chamber beneath the Aira caldera, to

^{*}Department of Geosystem Sciences, College of Humanities and Sciences, Nihon University, 3-25-40 Sakurajyosui Setagayaku, Tokyo 156-8550, Japan.

^{**}Graduate School of Science and Technology, Ibaraki University, 2-1-1 Bunkyo, Mito 310-8512, Japan.

^{***}Department of Earth Sciences, Faculty of Science, Ibaraki University, 2-1-1 Bunkyo, Mito 310-8512, Japan.

^{****}Graduate School of Integrated Basic Sciences, Nihon University, 3-25-40 Sakurajyosui Setagayaku, Tokyo 156-8550, Japan.

^{*****}Graduate School of Science and Technology, Kagoshima University, 1-21-35 Korimoto, Kagoshima 890-0055, Japan.

^{*****}Sakurajima Volcano Research Center, Disaster Prevention Research Institute, Kyoto University, Sakurajima-Yokoyamacho, Kagoshima 891-1419, Japan.

Corresponding author: Masaki Takahashi
e-mail: takahashi.masaki@nihon-u.ac.jp

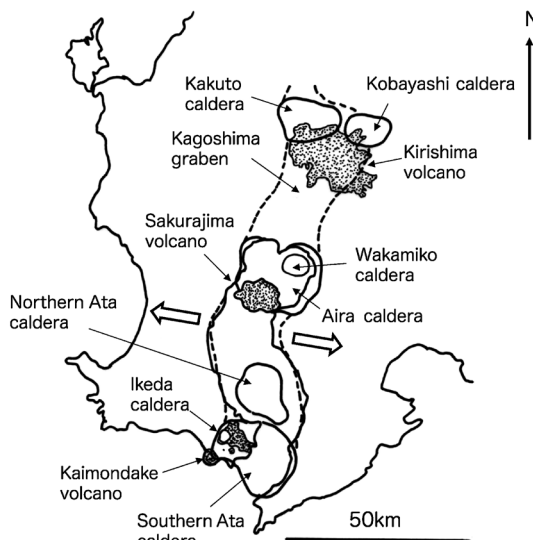


Fig. 1. Map showing the distribution of the late Quaternary calderas in southern Kyushu and the location of the Aira caldera and Sakurajima volcano. Arrows indicate that the N-S trending Kagoshima graben is extending in E-W direction at rates of less than 7 to 8 mm/year.

which the magma is supplied at a rate of about $0.01 \text{ km}^3 / 10\text{years}$ (Iguchi, 2007; Hyadati *et al.*, 2008), showing that the magma chamber system of the Sakurajima volcano is closely related to that of the Aira caldera. Although the formation of the Aira caldera was completed by the large-scale eruption of the Osumi pumice fall, Ito pyroclastic flow and AT ash fall deposits at 29 ka, the onset of the formation of the Aira caldera goes back to at least 100 ka. The explosive eruptions of the felsic magma have been repeated since 100 ka in the Aira caldera. In this paper, the whole-rock major element, incompatible trace element and rare earth element chemistry of the eruptive products of the Sakurajima volcano and Aira caldera region since 61 ka are summarized and the evolution of magma chamber systems beneath the Aira caldera including the Sakurajima volcano since 61 ka will be discussed based on the whole-rock chemistry.

The ages mentioned in this paper include both the reported calendar/calibrated ^{14}C ages and those by the K-Ar radiometric datings.

2. Eruptive history of the Sakurajima Volcano and Aira Caldera

The Aira caldera is situated at the northern end of the Kagoshima (Kinkowan) bay, which comprises the southern half of the Kagoshima graben. The north-south trending Kagoshima graben extends about 100 km in length with a width of about 20 km, having been formed under the east-

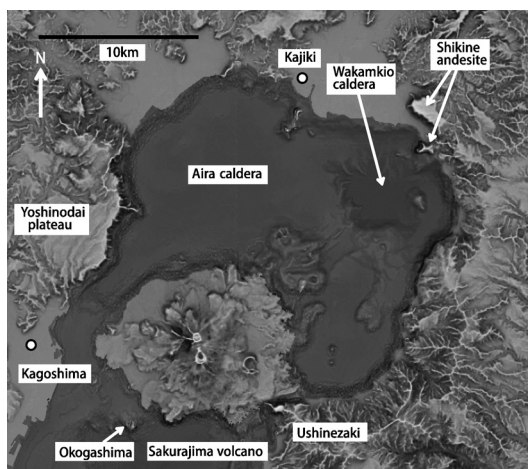


Fig. 2. The topographic relief map of the Aira caldera and Sakurajima volcano (courtesy of Chiba, T.). The Sakurajima volcano is located on the southern rim of the Aira caldera. The depression in the northeast portion of the caldera floor is the Wakamiko caldera. A rise in the western rim of the Aira caldera is the Yoshinodai plateau which consists of Quaternary volcanic rocks. A large hill near the north of the Wakamiko caldera comprises thick lavas of the Shikine andesite.

west extensional tectonics (Nagaoka, 1988), and its active extension is ongoing at rates of less than 7 to 8 mm/year (Wallace *et al.*, 2009) (Fig. 1).

The volcanic activity of the Aira caldera region since 1 Ma began with the eruption of andesitic to rhyolitic lavas at the Yoshinodai plateau in the western margin of the Aira caldera (Fig. 2), which was active during the time span from 1.0 to 0.8 Ma; they are the Kennooka pyroxene andesite, the Muregaoka pyroxene andesite, the Ryugamizu pyroxene andesite, the Amagahana hornblende dacite and the Mifune pyroxene rhyolite (Sudo *et al.*, 2000a; 2000b; 2001). The Yuwandake pyroxene andesite erupted from 0.9 to 0.5 Ma at the Kajiki area in the northern margin of the Aira caldera (Sudo *et al.*, 2000) (Fig. 2).

Around 0.5 Ma, the Osakibana pyroxene dacite, the Hiramatsu pyroxene andesite and the Shirahama basalt effused in the Yoshinodai plateau. The Yoshino hornblende pyroxene dacitic pyroclastic flow deposit erupted at 0.40 to 0.45 Ma near the Yoshinodai plateau, which is overlain by the Nanayashiro basalt effused at 0.35 Ma (Sudo *et al.*, 2000a; 2000b; 2001). The Ushine basalt erupted at 0.37 Ma at the Ushine area in the southern margin of the Aira caldera, and the Okogashima pyroxene rhyolite, now constructing a small island in the Kagoshima bay, effused at 0.38–0.25 Ma in the south of the present Sakurajima volcano (Tatsumi and Inoue, 1993) (Fig. 2).

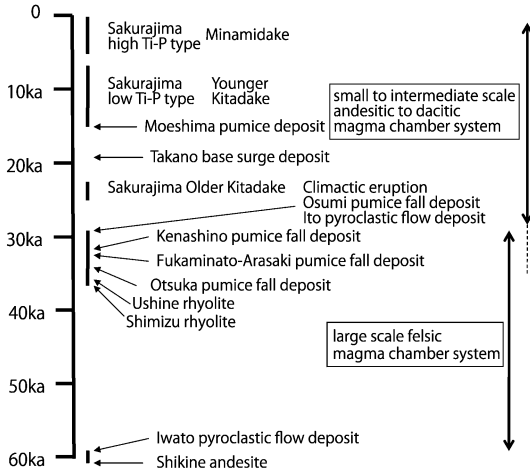


Fig. 3. History of the volcanic activity of the Sakurajima volcano and Aira caldera region since 61 ka.

The volcanic activity was nearly quiescent from 0.30 to 0.10 Ma and resumed at 0.10 Ma in the Aira caldera area; the eruptive style dramatically changed from effusive to explosive since 0.10 Ma (Nagaoka *et al.*, 2001). The eruption of the Hikiyama andesitic scoria fall deposit (103–95 ka) and the Kongoji pyroclastic surge deposit (95–86 ka) were followed by the large-scale explosive eruption of the Fukuyama hornblende pyroxene dacitic pumice fall deposit (40 km³) at about 90 ka (Nagaoka *et al.*, 2001).

The history of volcanic activity in the Sakurajima volcano–Aira caldera region since 61 ka is briefly summarized in Fig. 3. At the Kokubu area in the northeastern margin of the Aira caldera, the Shikine andesite (olivine bearing orthopyroxene clinopyroxene andesite to basaltic andesite) effused to produce thick lava flows with a total volume of 1.3 km³ at 61 ka (Nagaoka *et al.*, 2001; Sudo *et al.*, 2000ab). The Shikine andesite includes basaltic magmatic inclusions. The Iwato pyroclastic flow deposit (18–23 km³) with pyroxene rhyolitic pumice and andesitic scoria, consisting of the three pumice fall and five pyroclastic flow deposits, erupted at 60 ka probably from the northeastern portion in the Aira caldera (Nagaoka *et al.*, 2001). The scoria of the Iwato pyroclastic flow deposit is olivine bearing pyroxene andesite (Takahashi *et al.*, 2011).

The Shimizu hornblende pyroxene rhyolitic lava effused at 36 ka in the northern margin of the Aira caldera near the Kajiki city (Sudo *et al.*, 2000a; 2000b). The Ushine pyroxene rhyolitic lava erupted at 33 ka at the Ushine area in the southern margin of the Aira caldera (Sudo *et al.*, 2000a; 2000b). In the boring core samples drilled at the southern and southeastern portion of the Sakurajima volcano, the pyroxene andesite of 38 ka was found in the

depth of –98 m at the Furusato drill hole site and the pyroxene andesite of 30 ka was collected in the depth of –105 m at the Kurokami drill hole site (Miki *et al.*, 1999; 2000; 2003) (Fig. 4).

The intermediate scale eruption of the Otsuka pyroxene rhyolitic pumice fall deposit (32.5 ka; 0.9 km³), the Fukaminato–Arasaki pyroxene rhyolitic pumice fall and pyroclastic flow deposits (31 ka; 7.5 km³), and the Kenashino pyroxene rhyolitic pumice fall deposit (30 ka; 0.4 km³) were the precursors of the forthcoming climactic large-scale eruption (Nagaoka *et al.*, 2001).

At 29 ka, the climactic large-scale eruption of the pyroxene rhyolitic magma produced the Osumi pumice fall, Tarumizu pyroclastic flow, Tsumaya pyroclastic flow, Ito pyroclastic flow and AT ash fall deposits with a total volume of 450 km³ (Machida and Arai, 2003; Fukushima and Kobayashi, 2000) which completed the formation of the present Aira caldera (Aramaki, 1984). Although the precise location of the center of the climactic eruption has not yet been revealed, the Osumi pumice fall and Tarumizu pyroclastic flow deposits are estimated to have erupted from the location of the present Sakurajima volcano (Aramaki, 1984; Fukushima and Kobayashi, 2000), and the Wakamiko caldera, occupied the northeastern portion of the Aira caldera, is one of the probable candidates of the vent area of the Tsumaya and Ito pyroclastic flow deposits.

The construction of the Sakurajima volcano began at 26 ka in the southern margin of the Aira caldera after a dormant period of about three thousands of years (Kobayashi and Ezaki, 1997; Okuno, 1997 and 2002) (Fig. 4). The Sakurajima volcano is composed of the two main composite volcanic cones, the Kitadake situated in the north and the Minamidake in the south (Fig. 4). The volcanic history of the Sakurajima volcano comprises the three main stages, the older Kitadake (26 to 24 ka), younger Kitadake (13 to 4 ka) and Minamidake stages (4 ka to present) (Kobayashi and Ezaki, 1997; Okuno, 1997; 2002).

The three Plinian pumice fall deposits, P17 (26 ka), P16 (25 ka) and P15 (24 ka), erupted during the older Kitadake stage (Okuno, 2002). At 19 ka, the Takano base surge deposit was discharged in the Aira caldera (Okuno, 2002). After a dormant period of about eleven thousands of years, the younger Kitadake stage began with the eruption of the Satsuma pumice fall deposit (P14) at 12.8 ka, the eruptive volume of which is 2.5 km³ and it is the largest single eruptive event of the Sakurajima volcano (Moriwaki, 1992). Concurrently, the subaqueous eruption of the Shinshima (Moejima) pyroxene rhyolitic pumice occurred in the Aira caldera at 12.8 ka (Kano *et al.*, 1996; Okuno, 2002).

In the younger Kitadake stage, the nine Plinian pumice fall deposits, P13, P12, P11 (8 ka), P10 (7.7 ka), P9 (7.5 ka), P8 (6.5 ka), P7 (5 ka), P6 (3.8 ka), P5 (5.6 ka) erupted during the time span from 12.8 to 3.8 ka (Kobayashi and

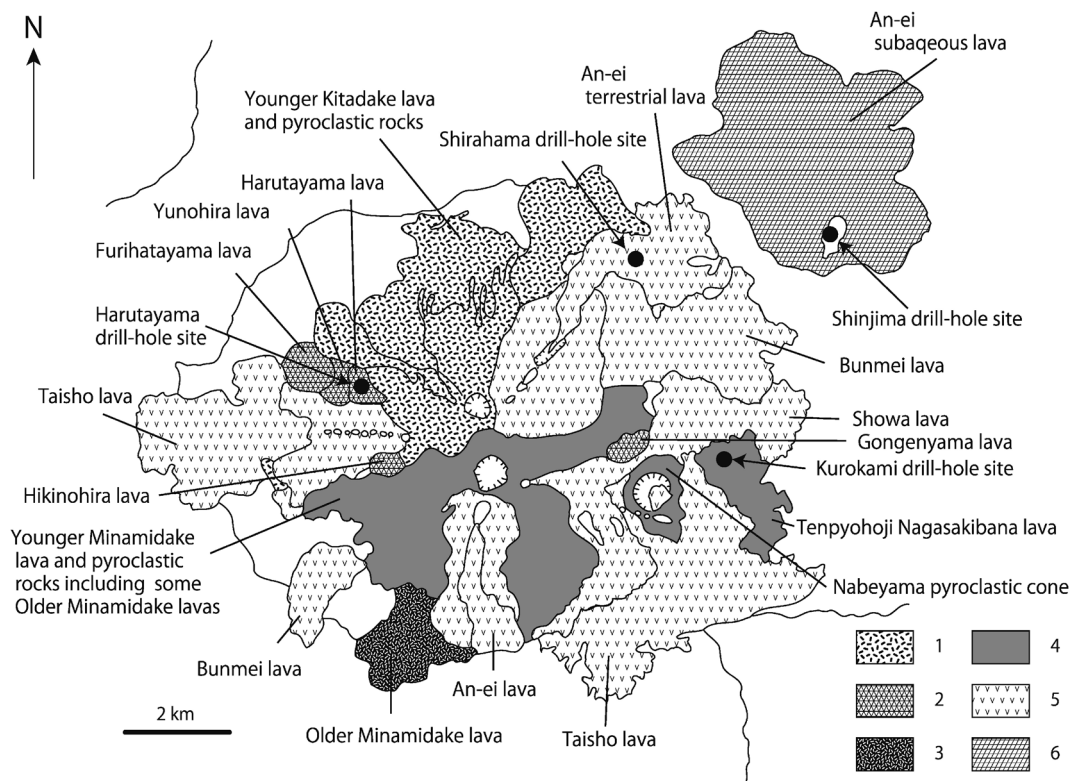


Fig. 4. Geologic sketch map showing the distribution of lavas and volcanic edifices of the Sakurajima volcano. 1: volcanic rocks of younger Kitadake; 2: lateral volcanoes of younger Kitadake; 3: Minamidake older lavas; 4: Minamidake younger, Nakadake and Tenpyohoji volcanic rocks; 5: Bunmei, An-ei terrestrial, Taisho and Showa volcanic rocks; 6: An-ei subaqueous volcanic rocks.

Ezaki, 1997; Okuno, 2002). The essential part of the present Kitadake volcanic cone was built during the younger Kitadake stage. Some of the younger Kitadake pyroxene dacitic lavas flowed down at about 10 ka and spread over the northern foot of the Kitadake volcanic cone (Miki *et al.*, 2003). The Gongenyama pyroxene dacitic lava dome in the eastern flank of the Kitadake volcanic cone was formed at 8 ka (Kobayashi and Ezaki, 1997), and the Harutayama pyroxene dacitic lava dome (including the Yunohira and Furihatayama lava domes) in the western flank of the Kitadake volcanic cone emerged at 7 ka (Uto *et al.*, 1999) (Fig. 4). One of the youngest pyroclastic flow deposit of the Kitadake volcanic cone erupted at 5 ka (Kobayashi and Ezaki, 1997), indicating that the construction of the main portion of the Kitadake volcanic cone was almost completed until 5 ka.

The Sakurajima volcanic ash deposit shows that the construction of the Minamidake volcanic cone by the frequent Vulcanian eruptions commenced at 4.5 ka and continued to 1.6 ka (Kobayashi and Ezaki, 1997). The older Minamidake andesitic lavas in the southern foot of the Minamidake pyroclastic cone effused during the period

from 4.0 to 3.7 ka (Miki, 1999) (Fig. 4).

The historical volcanic activity of the Minamidake volcano started from the Tenpyohoji eruption at 764 to 766AD, which occurred in the eastern flank of the Minamidake volcanic cone and produced the Tenpyohoji pumice fall deposit (P4), the Nabeyama pumice cone and the Nagasakibana pyroxene andesitic lava flow (Fig. 4). The Minamidake younger pyroxene dacitic lavas and the Nakadake volcanic edifice located between the Kitadake and Minamidake craters erupted between 8th and 12th centuries (Kobayashi and Ezaki, 1997; Kobayashi, 2010).

The Bunmei eruption at 1471 to 1476AD gave rise to the Bunmei pumice fall deposit (P3) and Bunmei pyroxene dacitic lava flows, the vent of which located in the northern and southern flanks of the Sakurajima volcano (Fig. 4). The An-ei eruption at 1779 to 1782AD comprises both the terrestrial and subaqueous eruptions; the An-ei terrestrial eruption produced the An-ei pumice fall deposit (P2) and An-ei pyroxene dacitic lava flows, while the An-ei subaqueous eruption formed the subaqueous pyroxene dacitic lava domes and cryptodomes, some of which appeared above the sea level as the An-ei islets

(Kobayashi, 2009) (Fig. 4). The An-ei terrestrial eruption occurred in the northern and southern flanks of the Sakurajima volcano.

The Taisho eruption at 1914 to 1915AD began with the Plinian eruption producing the Taisho pumice fall deposit (P1) and followed by the outpouring of the Taisho olivine bearing pyroxene andesitic lava flows, some of which is clastogenic in origin (Yasui *et al.*, 2007; 2013) (Fig. 4). The Taisho eruption occurred in the eastern and western flanks of the Sakurajima volcano. At 1946AD, the Showa olivine bearing pyroxene andesitic lava flow effused from the newly formed Showa crater located at the eastern upper slope of the Minamidake volcanic cone (Fig. 4). In the history of the Sakurajima volcano, the effusion of the Showa olivine bearing pyroxene andesitic lava is the latest event erupting lava flow.

3. Previous works

The whole-rock chemistry of the eruptive products of the Sakurajima volcano was firstly summarized by Yamaguchi (1974). Yamaguchi (1974) gave the 75 analytical data of major element chemistry of the volcanic rocks of the Sakurajima volcano, but did not discuss their petrology. Kurasawa *et al.* (1984) reported for the first time the Sr isotopic ratios of the Ito pyroclastic flow deposit, the AT ash fall deposit and some of the eruptive products of the Sakurajima volcano. According to Kurasawa *et al.* (1984), the $^{87}\text{Sr}/^{86}\text{Sr}$ ratios of the Ito pyroclastic flow and AT ash fall deposits are 0.7060 to 0.7062, while those of the younger Kitadake lavas, the Nabeyama pyroclastic cone of the Tenpyohoji eruption, the Bunmei and An-ei lavas, and the Taisho and Showa lavas of the Sakurajima volcano are 0.7054 to 0.7057, 0.7052, 0.7054 and 0.7053, respectively. Tsukui and Aramaki (1990) studied the whole-rock major and trace element chemistry of the eruptive products of the Osumi pumice fall and Ito pyroclastic flow deposits. They concluded that the erupted voluminous magma is high silica rhyolite and monotonous in composition.

Yanagi *et al.* (1991) examined in detail about the chemical composition of phenocrystic minerals of the lavas of the historic large-scale eruption of the Sakurajima volcano. The core anorthite compositions (An) of phenocrystic plagioclase of the Taisho and Showa lavas show bimodal distribution, while those of the Bunmei and An-ei lavas are almost unimodal. The orthopyroxene and clinopyroxene phenocryst of the Taisho and Showa lavas show reverse zoning, but those of the Bunmei and An-ei lavas mostly exhibit normal zoning. On the basis of above data, they advocated that the magmas of the Taisho and Showa eruptions suffered magma mixing; the dacitic magma with low An phenocrystic plagioclase and low Mg-number phenocrystic pyroxenes are mixed with the basaltic magma with high An phenocrystic plagioclase, high Mg-number phenocrystic pyroxenes and olivine. Contrarily, there are

no positive evidences of magma mixing in the magmas of the Bunmei and An-ei eruptions.

Arakawa *et al.* (1998) investigated the Sr and Nd isotopic ratios of the Osumi pumice fall and Ito pyroclastic flow deposits, the historical eruptive products of the Sakurajima volcano, and some of the volcanic rocks of the pre-Aira caldera, and discussed their origin. The $^{87}\text{Sr}/^{86}\text{Sr}$ isotopic ratios of the high-silica rhyolite producing the Osumi pumice fall and Ito pyroclastic flow deposits are 0.7052 to 0.7076, and those of the pre-caldera basalt and andesite are 0.7047 to 0.7054. They also threw light on the $^{87}\text{Sr}/^{86}\text{Sr}$ ratios of the historical lavas of the Sakurajima volcano; those of the Bunmei, An-ei, Taisho and Showa lavas are 0.7052 to 0.7053, 0.7052 to 0.7053, 0.7050 to 0.7053 and 0.7051 to 0.7052, respectively. Arakawa *et al.* (1998) concluded that the high-silica rhyolitic magma of the Osumi pumice fall and Ito pyroclastic flow deposits with relatively high $^{87}\text{Sr}/^{86}\text{Sr}$ ratios were produced by the partial melting of the lower crust, while the historical andesitic lavas of the Sakurajima volcano are the mixing products of the dacitic magma of lower crustal origin and the basaltic magma of mantle origin.

Arakawa *et al.* (1998) also presented the rare earth element (REE) contents of the Osumi pumice fall and Ito pyroclastic flow deposits, the historical eruptive products of the Sakurajima volcano, and some of volcanic rocks of the pre-Aira caldera stage. The pumice of the Osumi pumice fall and Ito pyroclastic flow deposits are enriched in light REE with high LREE/HREE ratio and shows negative Eu anomaly in the chondrite normalized diagram. The LREE/HREE ratio is modest in the andesite of the Sakurajima volcano, which shows slightly negative Eu anomaly, and the LREE/HREE ratio is the least in the basalt of the pre-Aira caldera stage, which has no Eu anomaly. The results of the REE analysis are consistent with their conclusion based on the Sr and Nd isotopic compositions that the andesite was formed by magma mixing between the crustal felsic magma and the basaltic magma of mantle origin.

Uto *et al.* (2005) studied the generation process of magmas of the Sakurajima volcano based on the Sr isotope, major and trace element compositions. Uto *et al.* (2005) showed that the eruptive products of the Sakurajima volcano older than 2 ka are poorer in TiO_2 , P_2O_5 , FeO^* , Na_2O , Zr and Y, and lower in Nb/Th and Zr/Th ratios than those younger than 2 ka. The $^{87}\text{Sr}/^{86}\text{Sr}$ ratios of the volcanic rocks older than 2 ka are 0.7055 to 0.7057 and those younger than 2 ka are 0.7051 to 0.7054. The rhyolite of the Ito pyroclastic flow deposit is higher in $^{87}\text{Sr}/^{86}\text{Sr}$ ratio (0.7060) and lower in Nb/Th and Zr/Th ratios, while the basaltic magmatic inclusion in the lavas of the Sakurajima volcano and the basalt to andesite of the pre-caldera stage are lower in the $^{87}\text{Sr}/^{86}\text{Sr}$ ratio (0.7049 to 0.7051) and higher in Nb/Th and Zr/Th ratios. Their conclusions are as follows; (1) magma mixing between the

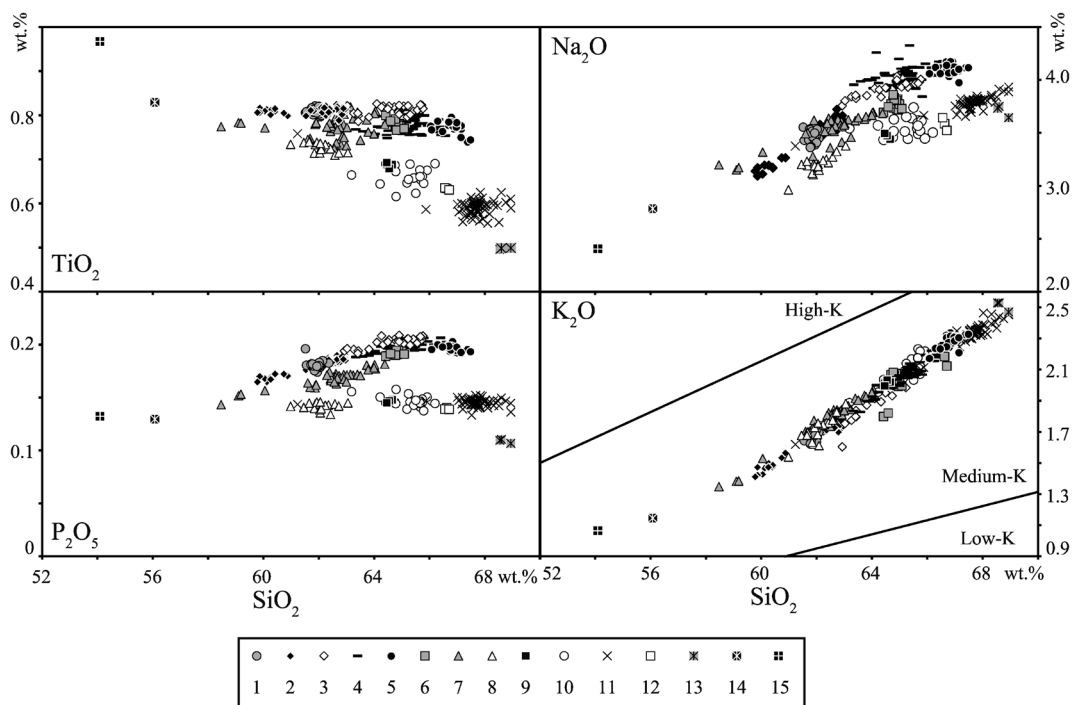


Fig. 5. Silica variation diagrams for TiO_2 , P_2O_5 , Na_2O and K_2O contents of the eruptive products of the Sakurajima volcano. 1: Showa lava; 2: Taisho lava; 3: An-ei subaqueous lava; 4: An-ei terrestrial lava; 5: Bunmei lava; 6: younger Minamidake lava; 7: Tenpyohoji lava; 8: older Minamidake lava; 9: younger Kitadake pyroclastic flow deposit; 10: younger Kitadake lava; 11: Furihatayama-Harutayama lava; 12: Hikinohira lava; 13: Gongenyama lava; 14: andesitic magmatic inclusion of the An-ei terrestrial lava (Yanagi *et al.*, 1991); 15: basaltic andesitic magmatic inclusion of the younger Kitadake lava.

felsic magma, being erupted as the Ito pyroclastic flow deposit, and the mafic magma, producing the basaltic magmatic inclusions in the lavas of the Sakurajima volcano and the basalt of the pre-caldera stage, gave rise to the andesite and dacite of the Sakurajima volcano, and (2) the mixing ratio of the mafic magma to felsic magma increased with time from the eruptions older than 2 ka to those younger than 2 ka.

4. Major element

The whole-rock major element chemistry of the eruptive products was obtained using the X-ray fluorescence spectrometry (XRF). All data were recalculated to 100% water-free. The table of analytical data and maps of sampling localities, in addition to the details of accuracy and method of chemical analysis, are shown in Takahashi *et al.* (2011). The data of the chemical analysis include those of the boring core samples of the Kurokami (the Tenpyohiji Nagasakibana lava), Shirahama (the An-ei terrestrial and younger Kitadake lavas), Shinjima (the An-ei subaqueous lava) and Harutayama (the Harutayama lava) drill-hole sites.

4-1 Sakurajima volcano

The eruptive products of the Sakurajima volcano are classified into the two types based on the TiO_2 and P_2O_5 contents; they are the high Ti-P and low Ti-P types (Fig. 5). The historic eruptive products are the high Ti-P types, while the pre-historic ones belong to the low Ti-P types. The historic eruptive products include the Tenpyohoji (Nagasakibana) (58 to 64 wt.% SiO_2), younger Minamidake (64 to 65 wt.% SiO_2), Bunmei (66 to 68 wt.% SiO_2), An-ei terrestrial (63 to 66 wt.% SiO_2), An-ei subaqueous (63 to 65 wt.% SiO_2), Taisho (59 to 62 wt.% SiO_2) and Showa (61 to 62 wt.% SiO_2) lavas. On the other hand, the pre-historic eruptive products include the older Minamidake (61 to 63 wt.% SiO_2), younger Kitadake (63 to 65 wt.% SiO_2), Hikinohira (66 wt.% SiO_2), Furihatayama-Harutayama (67 to 68 wt.% SiO_2) and Gongenyama (68 wt.% SiO_2) lavas.

The high Ti-P types are enriched in TiO_2 , P_2O_5 , Na_2O and FeO^* and depleted in MgO , Al_2O_3 and CaO , while the low Ti-P types are lower in TiO_2 , P_2O_5 , Na_2O and FeO^* , and higher in MgO , Al_2O_3 and CaO (Fig. 5 and 6). The K_2O contents of both types are similar and belong to the

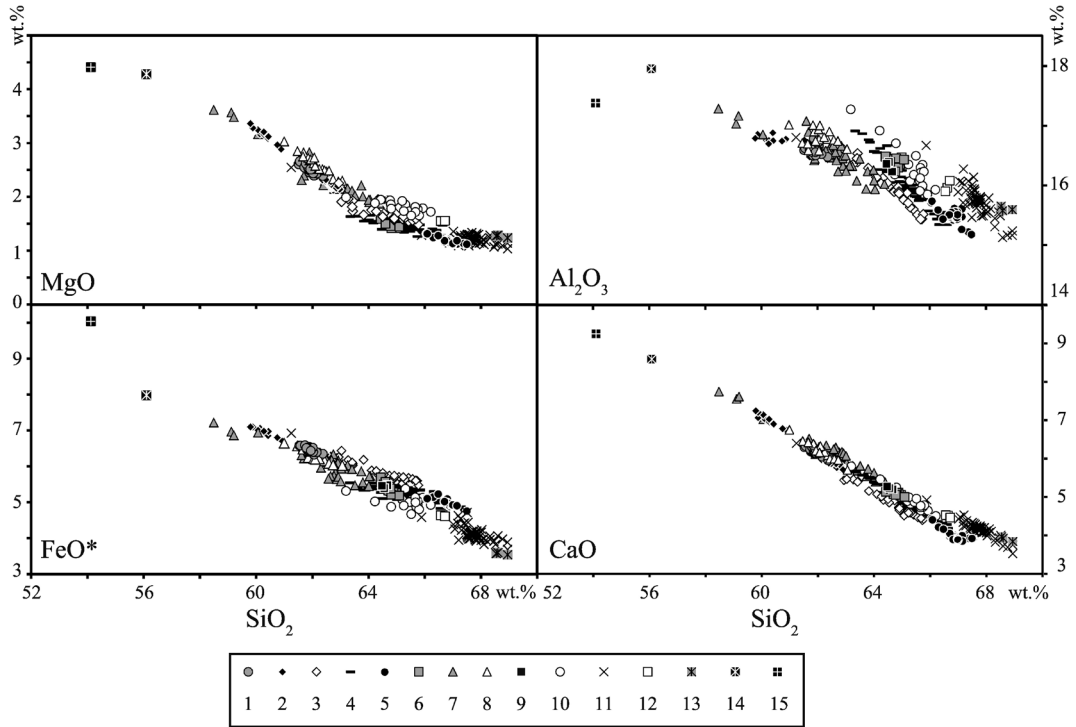


Fig. 6. Silica variation diagrams for MgO, FeO*, Al₂O₃ and CaO of the eruptive products of the Sakurajima volcano. 1: Showa lava; 2: Taisho lava; 3: An-ei subaqueous lava; 4: An-ei terrestrial lava; 5: Bunmei lava; 6: younger Minamidake lava; 7: Tenpyohoji lava; 8: older Minamidake lava; 9: younger Kitadake pyroclastic flow deposit; 10: younger Kitadake lava; 11: Furihatayama-Harutayama lava; 12: Hikinohira lava; 13: Gongenyama lava; 14: andesitic magmatic inclusion of the An-ei terrestrial lava (Yanagi *et al.*, 1991); 15: basaltic andesitic magmatic inclusion of the younger Kitadake lava.

Gill's medium-K series (Fig. 5). The TiO₂ contents of the high Ti-P types are nearly constant with increase of SiO₂, while those of the low Ti-P types decrease. The P₂O₅ contents of the high Ti-P types increase with increase of SiO₂, but those of the low Ti-P types are nearly constant. In both types, MgO, FeO*, Al₂O₃, CaO, and MnO contents decrease but K₂O and Na₂O contents increase with increasing SiO₂ in the silica variation diagrams (Fig. 5 and 6).

Mafic magmatic inclusions (MMI) are found in some lavas, such as the An-ei and younger Kitadake lavas; those in the high Ti-P type An-ei lava are mafic andesitic (ca.56 wt.%SiO₂) (Yanagi *et al.*,1991) and those in the low Ti-P type younger Kitadake lava are basaltic andesitic (ca. 54 wt.%SiO₂) in composition.

The high Ti-P types are further classified into the three sub-groups. The Tenpyohoji lava is the first sub-group and the second comprises the younger Minamidake, Bunmei and terrestrial An-ei lavas, and the third consists of the subaqueous An-ei, Taisho and Showa lavas. The third sub-group is the highest in TiO₂, P₂O₅ and FeO*, while the first sub-group is the lowest in P₂O₅ and Na₂O

(Figs. 5 and 6). The younger Minamidake lava of the second sub-group is slightly lower in Na₂O than other members of the same sub-group. Among the low Ti-P types, the Gongenyama lava is lower in TiO₂ and P₂O₅ than others (Fig. 5).

In the FeO*/MgO vs. SiO₂ diagram, most lavas belong to the calc-alkaline rock-series except for the younger Minamidake, Bunmei, An-ei terrestrial, and An-ei subaqueous lavas, which are the tholeiitic rock-series (Fig. 7)

4-2 Iwato pyroclastic flow, Osumi pumice fall and Ito pyroclastic flow deposits and related pyroclastic rocks.

The pumice of the Iwato pyroclastic flow deposit (72 to 74 wt.%SiO₂) and the Moeshima pumice (71 to 73 wt.%SiO₂) are rhyolite in composition, and that of the Osumi pumice fall and Ito pyroclastic flow deposits is high-silica rhyolite (74 to 76 wt.%SiO₂) (Figs.8 and 9). The scoria of the Iwato pyroclastic flow deposit is andesite (57 to 59 wt.%SiO₂) (Figs. 8 and 9). The felsic essential clasts of the Iwato pyroclastic flow, Osumi pumice fall and Ito pyroclastic flow deposits show the same trend of compositional

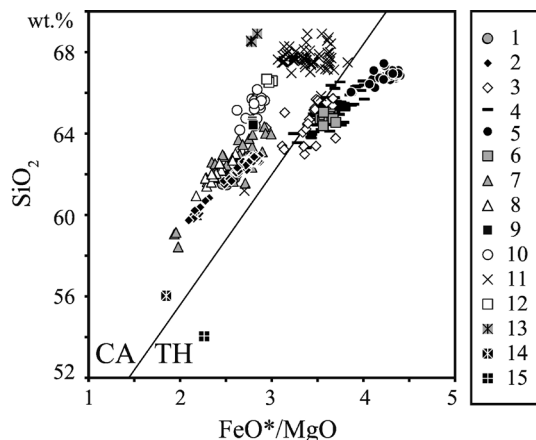


Fig. 7. SiO_2 vs. FeO^*/MgO diagram for the eruptive products of the Sakurajima volcano.

1: Showa lava; 2: Taisho lava; 3: An-ei subaqueous lava; 4: An-ei terrestrial lava; 5: Bunmei lava; 6: younger Minamidake lava; 7: Tenpyohoji lava; 8: older Minamidake lava; 9: younger Kitadake pyroclastic flow deposit; 10: younger Kitadake lava; 11: Furihatayama-Harutayama lava; 12: Hikinohira lava; 13: Gongenyama lava; 14: andesitic magmatic inclusion of the An-ei terrestrial lava (Yanagi *et al.*, 1991); 15: basaltic andesitic magmatic inclusion of the younger Kitadake lava.

variation in the silica variation diagrams. On the contrary, the Moeshima pumice is lower in TiO_2 , P_2O_5 , MgO , Al_2O_3 and CaO , and higher in Na_2O , K_2O , FeO^* and MnO than the Iwato pyroclastic flow, Osumi pumice fall and Ito pyroclastic flow deposits (Figs.8 and 9). The andesitic scoria of the Iwato pyroclastic flow deposit is higher in K_2O and lower in Na_2O , CaO and MnO than the andesite of the Sakurajima volcano (Figs.8 and 9).

In the FeO^*/MgO vs. SiO_2 diagram, the pumice and scoria of the Iwato pyroclastic flow deposit are the calc-alkaline rock-series and the pumice of the Osumi pumice fall and Ito pyroclastic flow deposits and the Moeshima pumice belong to the tholeiitic rock-series (Fig. 10). The pumice and scoria of the Iwato pyroclastic flow deposit, and the pumice of the Osumi pumice fall and Ito pyroclastic flow deposits are the Gill's medium-K series (Fig. 8).

4-3 Shikine andesite

The SiO_2 content of the Shikine andesite is 53 to 60 wt. %, which includes the basaltic MMI (51 wt.% SiO_2). The Shikine andesite is lower in P_2O_5 , Na_2O and MnO , compared with the andesite of the Sakurajima volcano (Fig. 8 and 9). The Shikine andesite belongs to the Gill's medium-K series on the K_2O vs. SiO_2 diagram and the calc-alkaline rock-series in the FeO^*/MgO vs. SiO_2 diagram (Fig. 10). The whole-rock major element chemistry

of the Shikine andesite is nearly the same as that of the scoria of the Iwato pyroclastic flow deposit except for P_2O_5 and K_2O contents (Figs.8 and 9). The basaltic MMI (about 52 wt.% SiO_2) is included in the Shikine andesite.

5. Incompatible trace element

The whole-rock incompatible trace element chemistry of the eruptive products is obtained by using the X-ray fluorescence spectrometry (XRF). The details of the analytical method and accuracy of the chemical analysis are presented in Takahashi *et al.* (2011).

The content of incompatible trace elements excluding Sr increases with increase of SiO_2 in the silica variation diagram.

The HFSE such as Zr and Nb, and Y contents of the high Ti-P types of the Sakurajima volcano are higher than those of the low Ti-P types in the silica variation diagram (Fig. 11). The rhyolitic pumice of the Iwato pyroclastic flow, Osumi pumice fall and Ito pyroclastic flow deposits are depleted in Zr, Nb and Y, compared with those of the Moeshima rhyolitic pumice (Fig. 11). The Shikine andesite and the andesitic scoria of the Iwato pyroclastic flow deposit are enriched in Rb, Ba and Nb, and depleted in Sr in the silica variation diagram, in comparison with other volcanic rocks of the Sakurajima volcano and Aira caldera region (Fig. 11).

The boring core samples consist of the Tenpyohoji (the Kurokami drill-hole site), An-ei terrestrial (the Shirahama drill-hole site), An-ei subaqueous (the Shinjima drill-hole site), younger Kitadake (the Shirahama drill-hole site) and Harutayama (the Harutayama drill-hole site) lavas. The Sr content of the Harutayama lava is the highest and that of the Tenpyohoji lava is the lowest, but the inclination of compositional trend of the Tenpyohoji lava is rather gentle in the silica variation diagram (Fig. 12). The lavas of the high Ti-P types, such as the Tenpyohoji, An-ei terrestrial, and An-ei subaqueous lavas, are rather enriched in Zr, Nb and Y in the silica variation diagrams, but some of the Tenpyohoji lava are lower in Nb (Fig. 12). The Zr content of the Harutayama lava, a member of the low Ti-P types, is higher than that of the younger Kitadake lava which is also a member of the low Ti-P types (Fig. 12). On the other hand, the Zr and Y contents of the An-ei subaqueous lava are higher than those of the An-ei terrestrial lava, although both are members of the high Ti-P types (Fig. 12).

The Rb/Zr , Rb/Y , Ba/Y and Zr/Y ratios of the pumice of the Iwato pyroclastic flow, Osumi pumice fall and Ito pyroclastic flow deposits are similar and higher than those of other volcanic rocks of the Sakurajima volcano and Aira caldera region since 61 ka (Fig. 13).

The Rb/Zr , Rb/Y , Ba/Y and Zr/Y ratios of the high Ti-P types of the Sakurajima volcano are lower than those of the low Ti-P types and the Moeshima rhyolitic pumice (Fig. 13). The Rb/Zr , Rb/Y , Ba/Y , and Zr/Y ratios of the basaltic MMI of the Shikine andesite and basaltic andesitic

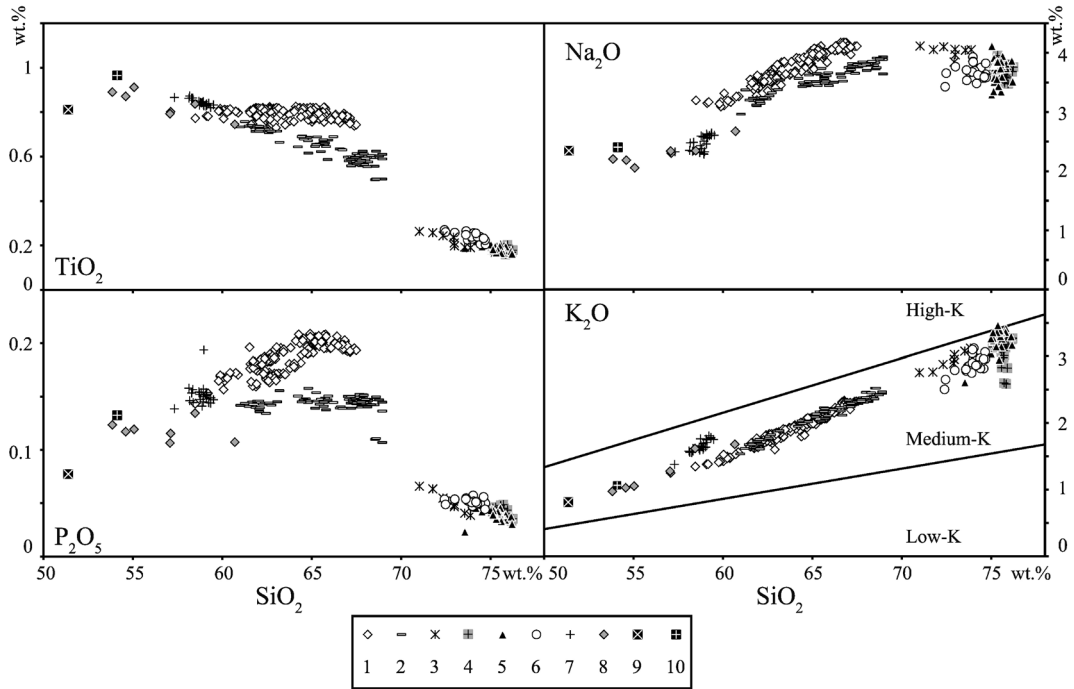


Fig. 8. Silica variation diagrams for TiO_2 and P_2O_5 , Na_2O and K_2O contents of the eruptive products of the Sakurajima volcano and Aira caldera region since 61 ka. 1: Minamidake historical lavas; 2: older Minamidake lava, lavas and pyroclastic flow deposit of Kitadake; 3: Moeshima pumice; 4: Osumi pumice fall deposit; 5: Ito pyroclastic flow deposit; 6: Iwato pyroclastic flow deposit (pumice); 7: Iwato pyroclastic flow deposit (scoria); 8: Shikine andesite; 9: basaltic magmatic inclusion of the Shikine andesite; 10: basaltic andesitic magmatic inclusion of the younger Kitadake lava.

MMI of the younger Kitadake lava, and those of the mafic andesite of the Shikine andesite are nearly constant and the lowest among the eruptive products of the Sakurajima volcano and Aira caldera region since 61 ka (Fig. 13). On the contrary, the Rb/Zr, Rb/Y, Ba/Y and Zr/Y ratios of the andesite of the Shikine andesite and the andesitic scoria of the Iwato pyroclastic flow deposit show wide variations (Fig. 13).

The boring core samples of the low Ti-P types, the younger Kitadake and Harutayama lavas, are higher in Rb/Y, Rb/Zr, Ba/Y and Zr/Y ratios than those of the historical Tenpyohoji, An-ei terrestrial and An-ei subaqueous lavas which belong to the high Ti-P types (Fig. 14). The boring core samples of the An-ei subaqueous lava are lower in Rb/Zr, Rb/Y, Ba/Y and Zr/Y ratios than those of the An-ei terrestrial lava.

6. Rare earth element

The whole-rock chemistry of rare earth elements is obtained by the inductively coupled plasma (ICP) analytical apparatus. The details of the analytical method and the accuracy of chemical analysis are presented in Tagiri and Fujinawa (1988).

The chondrite-normalized abundance of rare earth

elements (REE) of the high Ti-P and low Ti-P types of the Sakurajima volcano are intermediate between those of the pumice of the Moeshima pumice deposit and the basaltic MMI in the younger Kitadake lava of the Sakurajima volcano (Fig. 15). The LREE (Light REE)/HREE (Heavy REE) ratios are the highest in the Moeshima pumice deposit and the lowest in the basaltic andesitic MMI of the younger Kitadake lava (Fig. 15). The LREE/HREE ratios of the low Ti-P types are higher than those of the high Ti-P types of the Sakurajima volcano (Fig. 15).

The chondrite-normalized abundance of REE is lower in the pumice of the Iwato pyroclastic flow, Osumi pumice fall and Ito pyroclastic flow deposits and higher in the scoria of the Iwato pyroclastic flow deposit, the high Ti-P types and low Ti-P types of the Sakurajima volcano, and the pumice of the Moeshima pumice deposit (Fig. 16). The LREE/HREE ratios of the pumice of the Iwato pyroclastic flow, Osumi pumice fall and Ito pyroclastic flow deposits are higher than those of the scoria of the Iwato pyroclastic flow deposit, the high Ti-P types and low Ti-P types of the Sakurajima volcano, and the pumice of the Moeshima pumice deposit, although all of them show negative Eu anomaly (Fig. 16).

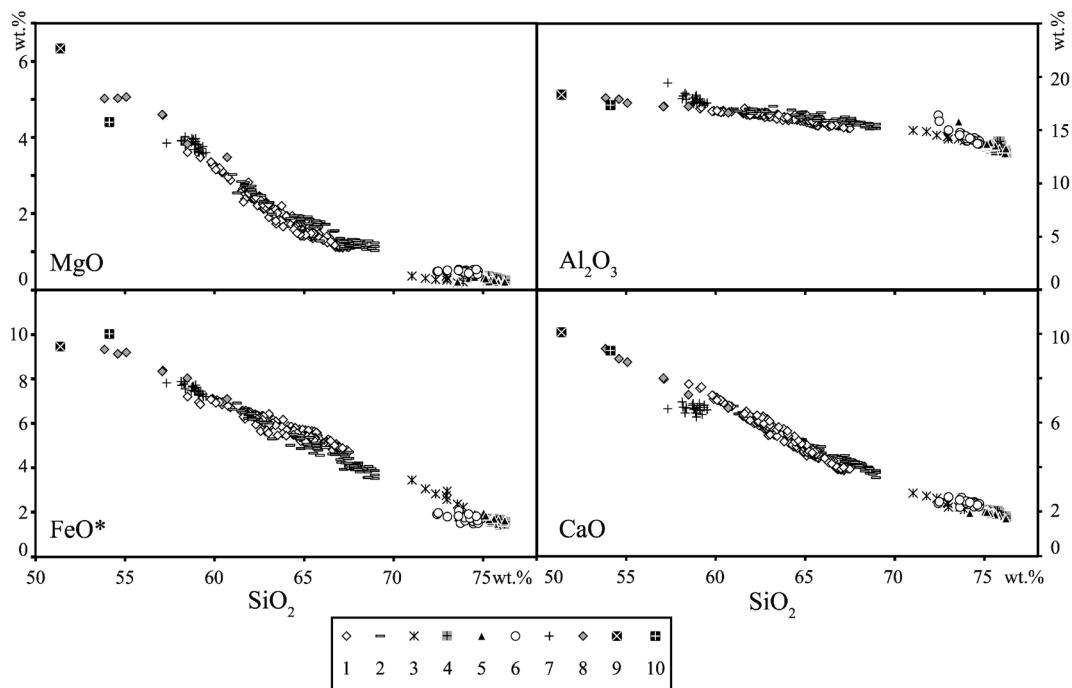


Fig. 9. Silica variation diagrams for MgO, FeO*, Al₂O₃ and CaO contents of the eruptive products of the Sakurajima volcano and Aira caldera region since 61 ka. 1: Minamidake historical lavas; 2: older Minamidake lava, lavas and pyroclastic flow deposit of Kitadake; 3: Moeshima pumice; 4: Osumi pumice fall deposit; 5: Ito pyroclastic flow deposit; 6: Iwato pyroclastic flow deposit (pumice); 7: Iwato pyroclastic flow deposit (scoria); 8: Shikine andesite; 9: basaltic magmatic inclusion of the Shikine andesite; 10: basaltic andesitic magmatic inclusion of the younger Kitadake lava.

7. Discussion

7-1 Origin of basaltic to basaltic andesitic magmas of the Sakurajima volcano and Aira caldera region since 61 ka

Basaltic to basaltic andesitic rocks are rare in the Sakurajima volcano and Aira caldera region since 61 ka; they occur only as the basaltic MMI and basaltic andesitic lava in the Shikine andesite and the basaltic andesitic MMI of the younger Kitadake lava of the Sakurajima volcano. They have nearly the same incompatible trace element ratios, and the basaltic andesite can be derived from the basaltic magma produced the basaltic MMI by the simple crystallization differentiation of olivine, pyroxenes and plagioclase, because MgO and CaO decrease and TiO₂, P₂O₅, K₂O, Rb, Ba, Nb and Y increase, while Al₂O₃, Na₂O and Sr are nearly constant as SiO₂ increases in the silica variation diagrams (Fig. 8, 9 and 11). The basaltic andesitic MMI in the younger Kitadake lava is, however, slightly higher in Na₂O, FeO* and MnO, and lower in MgO and Nb than the basaltic andesite of the Shikine andesite. Since the differences are minimal, it may be plausible that they were derived from the similar more primitive parental basaltic magma. The ⁸⁷Sr/⁸⁶Sr isotopic ratio of the basaltic andesitic MMI of the younger Kitadake lava is not

so high (0.70505), hence they were considered to be the mantle origin in the previous study (Uto *et al.*, 2005).

Although the occurrence of the basaltic to basaltic andesitic rocks are rare in the Sakurajima volcano and Aira caldera region since 61 ka, they must have underplated voluminously to the lower crust, supplying enough heat to melt the lower crust and to produce felsic magmas in the Aira caldera region since 61 ka. The presence of abundant felsic magma in the shallow crust may block the ascent of the basaltic to basaltic andesitic magma from the deeper level in the crust to the surface, which may be the main reason why basaltic to basaltic andesitic rocks are rare in the Sakurajima volcano and Aira caldera region.

7-2 Origin of andesitic magma of the Sakurajima volcano and Aira caldera region since 61 ka

The andesites with 56 to 63 wt% SiO₂ are not abundant in the Sakurajima volcano and Aira caldera region since 61 ka. Significant amount of andesite occurred in the Shikine andesite as lavas and in the Iwato pyroclastic flow deposit as scoria. In the Sakurajima volcano, most volcanic rocks are dacite (SiO₂ > 63 wt.%) excluding the P5 air-fall pumice deposit and some of the older Minamidake, Tenpyohoji, Taisho and Showa lavas, which are andesitic in composition (Takahashi *et al.*, 2011). The andesites of

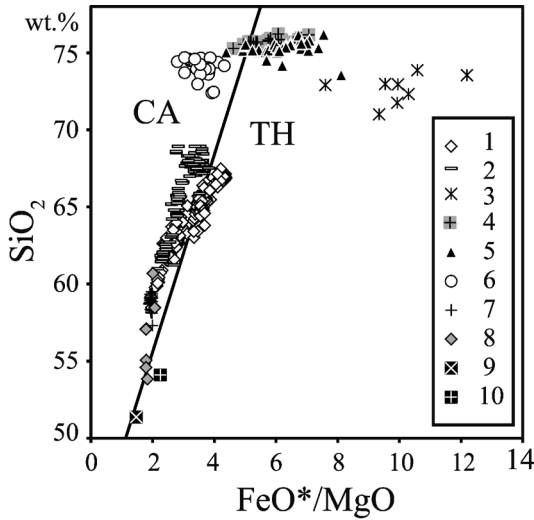


Fig. 10. SiO₂ vs. FeO*/MgO diagram for the eruptive products of the Sakurajima volcano and Aira caldera region since 61 ka. 1: Minamidake historical lavas; 2: older Minamidake lava, lavas and pyroclastic flow deposit of Kitadake; 3: Moeshima pumice; 4: Osumi pumice fall deposit; 5: Ito pyroclastic flow deposit; 6: Iwato pyroclastic flow deposit (pumice); 7: Iwato pyroclastic flow deposit (scoria); 8: Shikine andesite; 9: basaltic magmatic inclusion of the Shikine andesite; 10: basaltic andesitic magmatic inclusion of the younger Kitadake lava.

the Sakurajima volcano show the mineralogical evidences of magma mixing, such as reverse compositional zoning of plagioclase and pyroxenes (Yanagi *et al.*, 1991). The incompatible trace element ratios of andesites, such as Rb/Zr, Rb/Y, Ba/Y, and Zr/Y, show a wide range and their trends of variation are almost linear, suggesting that their trend of variation caused not by crystallization differentiation but by magma mixing of the end-member magmas with different incompatible trace element ratios.

For the Taisho and Showa lavas of the Sakurajima volcano, Yanagi *et al.* (1991) estimated that the mafic end-member magma is basaltic with 52 wt. %SiO₂ and the felsic end-member magma is dacitic with 69 wt. %SiO₂. The inclination of negative linear compositional trends of MgO content of the andesite of the high and low Ti-P types in the MgO vs. SiO₂ diagram are larger than those of the dacite of the high and low Ti-P types. Both compositional trends cross at around 65 wt%SiO₂ (Fig. 6), implying that the felsic end-member magmas of the andesite of the Sakurajima volcano are the dacite with around 65 wt. %SiO₂. Namely, the felsic end-member magma of the older Minamidake lavas, the Tenpyohoji lavas and the Taisho and Showa lavas are the dacite of the younger

Kitadake lava, the younger Minamidake lava, and the An-ei subaqueous lava, respectively, the SiO₂ contents of which are around 65 wt.%.

The compositions of mafic end-member magmas of andesitic magmas are inferred from the compositional trend of andesites in the silica variation diagrams. The extension of the linear compositional trends to the SiO₂ content corresponding to basalt to basaltic andesite suggests the composition of the mafic end-member magma. The inferred compositions of mafic end-member magma in the silica variation diagrams for Na₂O and Al₂O₃ are variable (Fig. 17). The estimated mafic end-member magma with high Na₂O is also high in Al₂O₃, suggesting that their compositional variations are mainly controlled by a series of crystallization differentiation of mafic minerals from a similar parental basaltic magma (Fig. 17).

The rhyolitic magma yielding the pumice of the Iwato pyroclastic flow deposit is a plausible candidate for the felsic end-member magma of the Shikine andesite (Fig. 18), but the felsic end-member magma of andesitic scoria of the Iwato pyroclastic flow deposit is not the rhyolitic magma of the Iwato pumice. The felsic end-member magma of the Iwato scoria must be more enriched in K₂O and Rb than the Iwato pumice. On the other hand, the mafic end-member magma of the andesitic scoria of the Iwato pyroclastic flow deposit was probably the mafic andesite or basaltic andesite of the Shikine andesite.

In the La/Yb vs. La diagram, it is also difficult to interpret the rhyolitic magma of the Iwato pyroclastic flow deposit as a candidate for felsic end-member magma of the andesitic scoria of the Iwato pyroclastic flow deposit (Fig. 19).

It may be concluded that the andesites with 56 to 63 wt%SiO₂ of the Sakurajima volcano and Aira caldera region since 61 ka are the products of magma mixing. The felsic end-member magma of the andesite of the Sakurajima volcano is dacitic, and that of the Shikine andesite are inferred to be the rhyolitic magma which produced the pumice of the Iwato pyroclastic flow deposit. The felsic end-member magma of the Iwato scoria is probably more enriched in K₂O and Rb than the Iwato pumice. The compositions of felsic end-member magma of andesite in the Sakurajima volcano and Aira caldera region since 61 ka are variable in each stage of volcanic activity.

7-3 Origin of felsic magmas of the Sakurajima volcano and Aira caldera region since 61 ka

The incompatible trace element ratios of the dacite and rhyolite of the Sakurajima volcano and Aira caldera region since 61 ka exhibit a wide range. The Rb/Y ratio, for example, is the highest in the pumice of the Iwato pyroclastic flow, Osumi pumice fall and Ito pyroclastic flow deposits, and the lowest in the dacitic members of the high Ti-P types of the Sakurajima volcano (Fig. 13). It is difficult to derive this wide range of Rb/Y ratios and other incompatible trace element ratios by simple crystallization

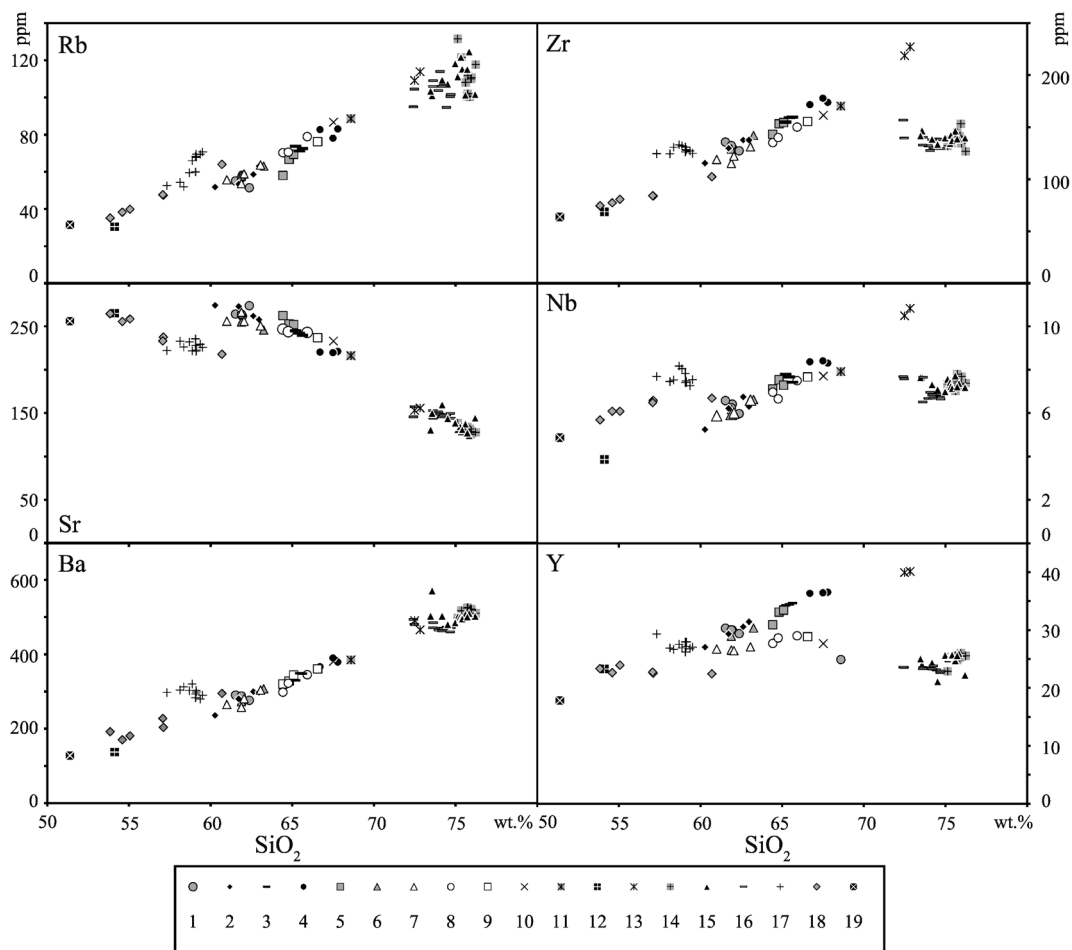


Fig. 11. Silica variation diagrams for Rb, Ba, Sr, Zr, Nb and Y contents of the eruptive products of the Sakurajima volcano and Aira caldera region since 61 ka. 1: Showa lava; 2: Taisho lava; 3: Anei terrestrial lava; 4: Bunmei lava; 5: younger Minamidake lava; 6: Tenpyohoji lava; 7: older Minamidake lava; 8: younger Kitadake lava; 9: Hikinohira lava; 10: Furihatayama lava; 11: Gongenyama lava; 12: mafic magmatic inclusion of the younger Kitadake lava; 13: Moeshima pumice; 14: Osumi pumice fall deposit; 15: Ito pyroclastic flow deposit; 16: Iwato pyroclastic flow deposit (pumice); 17: Iwato pyroclastic flow deposit (scoria); 18: Shikine andesite lava; 19: basaltic magmatic inclusion of the Shikine andesite.

differentiation of basaltic to basaltic andesitic magma; in the case of the Sakurajima volcano, the dacitic magmas cannot be produced by simple crystallization differentiation of basaltic andesitic magma, the composition of which is the same as the basaltic andesitic MMI of the younger Kitadake lava (Fig. 13). The wide range of the Rb/Y ratios also cannot be explained by magma mixing between the two end-members, for example the rhyolitic to high-silica rhyolitic magma producing the pumice of the Iwato pyroclastic flow, Osumi pumice fall and Ito pyroclastic flow deposits, and the basaltic to basaltic andesitic magma yielding the Shikine andesite or the basaltic andesitic MMI of the younger Kitadake lava of the

Sakurajima volcano (Fig. 13). The wide range of Rb/Y ratios of the felsic magmas suggests that their sources are different.

The Rb/Y ratios of felsic magmas decrease in the following order, (1) the rhyolitic to high-silica rhyolitic pumice of the Iwato pyroclastic flow, Osumi pumice fall and Ito pyroclastic flow deposits, (2) the Gongenyama dacitic lava of the younger Kitadake stage, (3) the Furihatayama-Harutayama dacitic lavas of the younger Kitadake stage, (4) the Moeshima rhyolitic pumice deposit, (5) the Hikinohira-Kitadake dacitic lavas of the younger Kitadake stage, (6) the dacitic lavas of the Minamidake stage (Fig. 13). The dacitic lavas of the

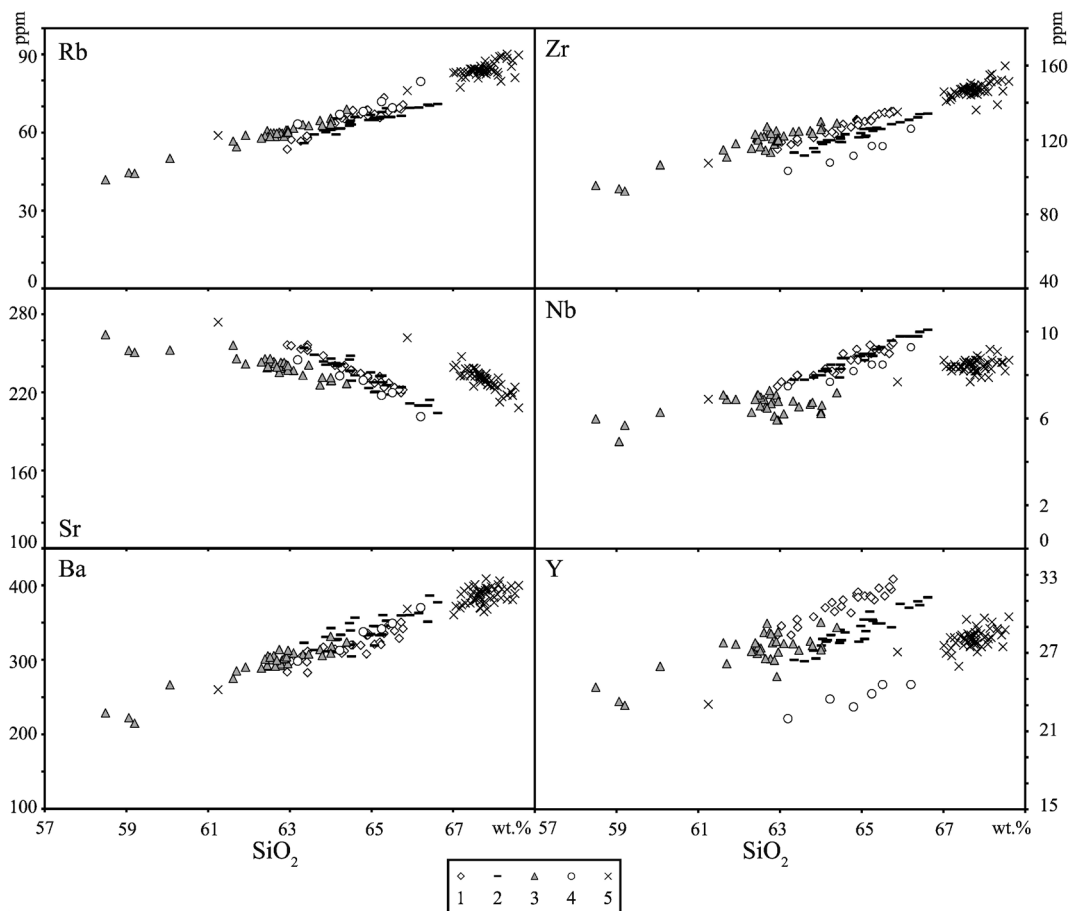


Fig. 12. Silica variation diagrams for Rb, Ba, Sr, Zr, Nb and Y contents of the lavas of boring core samples of drill-hole sites. 1: An-ei subaqueous lava; 2: An-ei terrestrial lava; 3: Tenpyohoji lava; 4: younger Kitadake lava; 5: Harutayama lava.

Minamidake stage are further classified into three sub-groups with different compositional trends based on Rb/Zr, Rb/Y, Ba/Y and Zr/Y ratios; they are (6-1) the An-ei terrestrial lavas, (6-2) the Tenpyohoji lava, and (6-3) the An-ei subaqueous lava (Fig. 14).

The high silica rhyolitic magma of the Osumi pumice fall and Ito pyroclastic flow deposits can be produced from the rhyolitic magma of the Iwato pyroclastic flow deposit by crystallization differentiation, because the incompatible trace element ratios of both magmas are similar and the content of incompatible trace element is lower in the rhyolitic magma of the Iwato pyroclastic flow deposit.

The chondrite-normalized patterns of REE of the pumice of the Iwato pyroclastic flow deposit and those of the Osumi pumice fall and Ito pyroclastic flow deposit are parallel and the REE is enriched in the Osumi pumice fall and Ito pyroclastic deposit, also indicating that the high-silica rhyolitic magma of the Osumi pumice fall and Ito

pyroclastic flow deposit can be derived from the rhyolitic magma producing pumice of the Iwato pyroclastic flow deposit by crystallization differentiation (Fig. 16).

The felsic magmas in the Sakurajima volcano and Aira caldera region since 61 ka probably comprise at least above eight types with different Rb/Y ratios, which could not be derived from the same source by the same process.

As regard to the Rb/Zr, Rb/Y, Ba/Y and Zr/Y ratios, it is also difficult to produce the felsic and andesitic magmas by crystallization differentiation of basaltic to basaltic andesitic magma, the composition of which is the same as the basaltic MMI of the Shikine andesite or the basaltic andesitic MMI of the younger Kitadake lava (Fig. 13).

The La/Yb ratios also range widely in the La/Yb vs. La diagram (Fig. 19). The La/Yb ratio is the highest in the pumice of the Iwato pyroclastic flow, Osumi pumice fall and Ito pyroclastic flow deposits, next in the low Ti-P types, and the lowest in the high Ti-P types of the

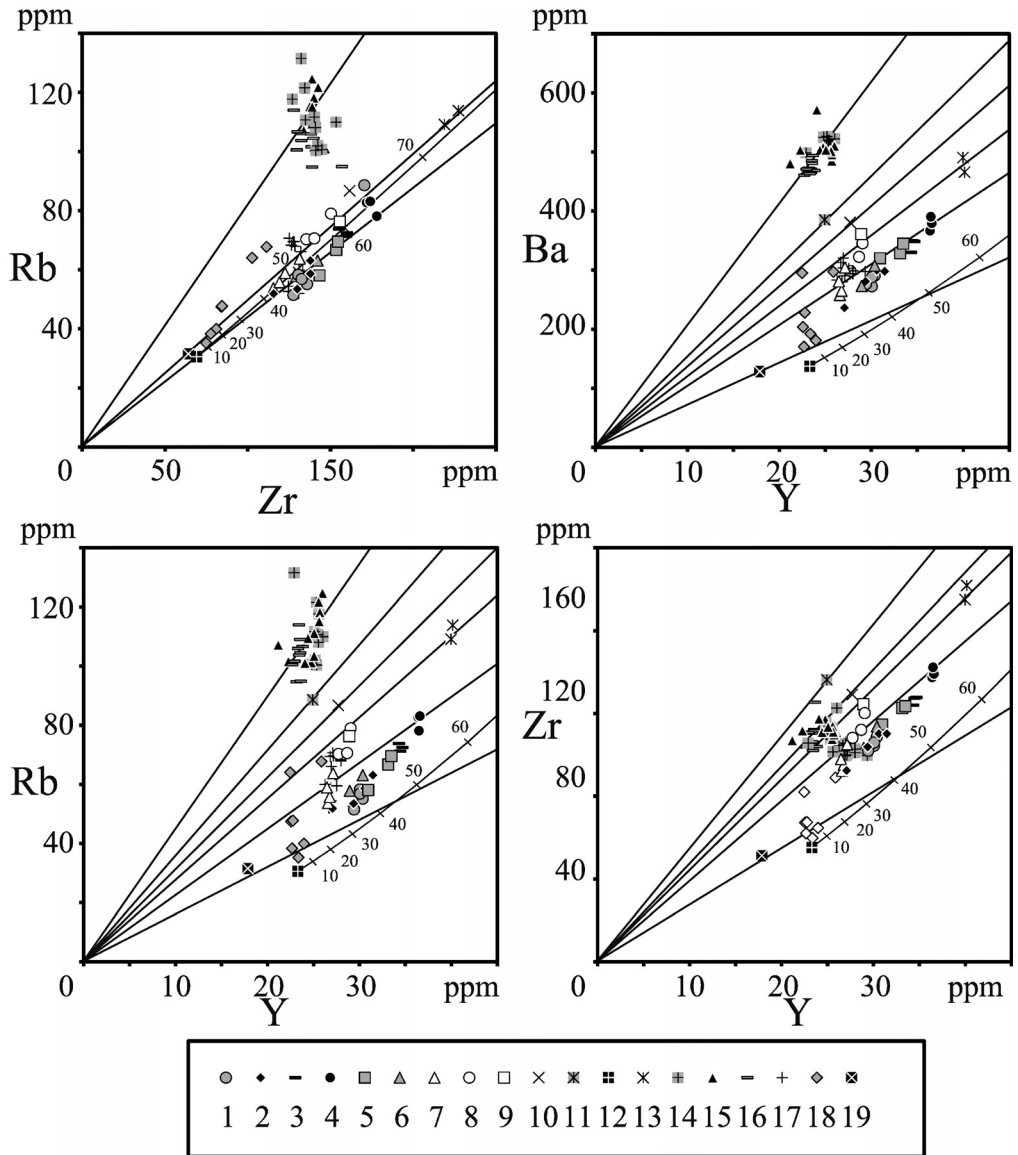


Fig. 13. Diagrams showing the incompatible trace element ratios of the eruptive products of the Sakurajima volcano and Aira caldera region since 61 ka with calculated crystallization differentiation trend started from the composition of the basaltic andesitic magmatic inclusion of the younger Kitadake lava. The partition coefficients of Rb, Zr and Y between minerals and basaltic magma are cited from Rollinson (1993). The crystallization differentiation trends are calculated based on the Rayleigh fractionation model using above partition coefficients and the modal composition of phenocrysts of the basaltic andesitic magmatic inclusion (plagioclase: 8.1vol.%; clinopyroxene: 7.3vol.%; orthopyroxene: 2.7vol.%; magnetite: 4.7vol.%; groundmass: 77.3vol. %). The simple crystallization differentiation of basaltic andesitic magma, represented by the composition of the magmatic inclusion of the younger Kitadake lava, cannot explain the wide range of ratios of the andesitic to felsic eruptive products of the Sakurajima volcano and Aira caldera region since 61 ka. A: Rb/Zr; B: Rb/Y; C: Ba/Y; D: Zr/Y. 1: Showa lava; 2: Taisho lava; 3: Anei terrestrial lava; 4: Bunmei lava; 5: younger Minamidake lava; 6: Tenpyohoji lava; 7: older Minamidake lava; 8: younger Kitadake lava; 9: Hikinohira lava; 10: Furihatayama lava; 11: Gongenyama lava; 12: mafic magmatic inclusion of the younger Kitadake lava; 13: Moeshima pumice; 14: Osumi pumice fall deposit; 15: Ito pyroclastic flow deposit; 16: Iwato pyroclastic flow deposit (pumice); 17: Iwato pyroclastic flow deposit (scoria); 18: Shikine andesite lava; 19: basaltic magmatic inclusion of the Shikine andesite.

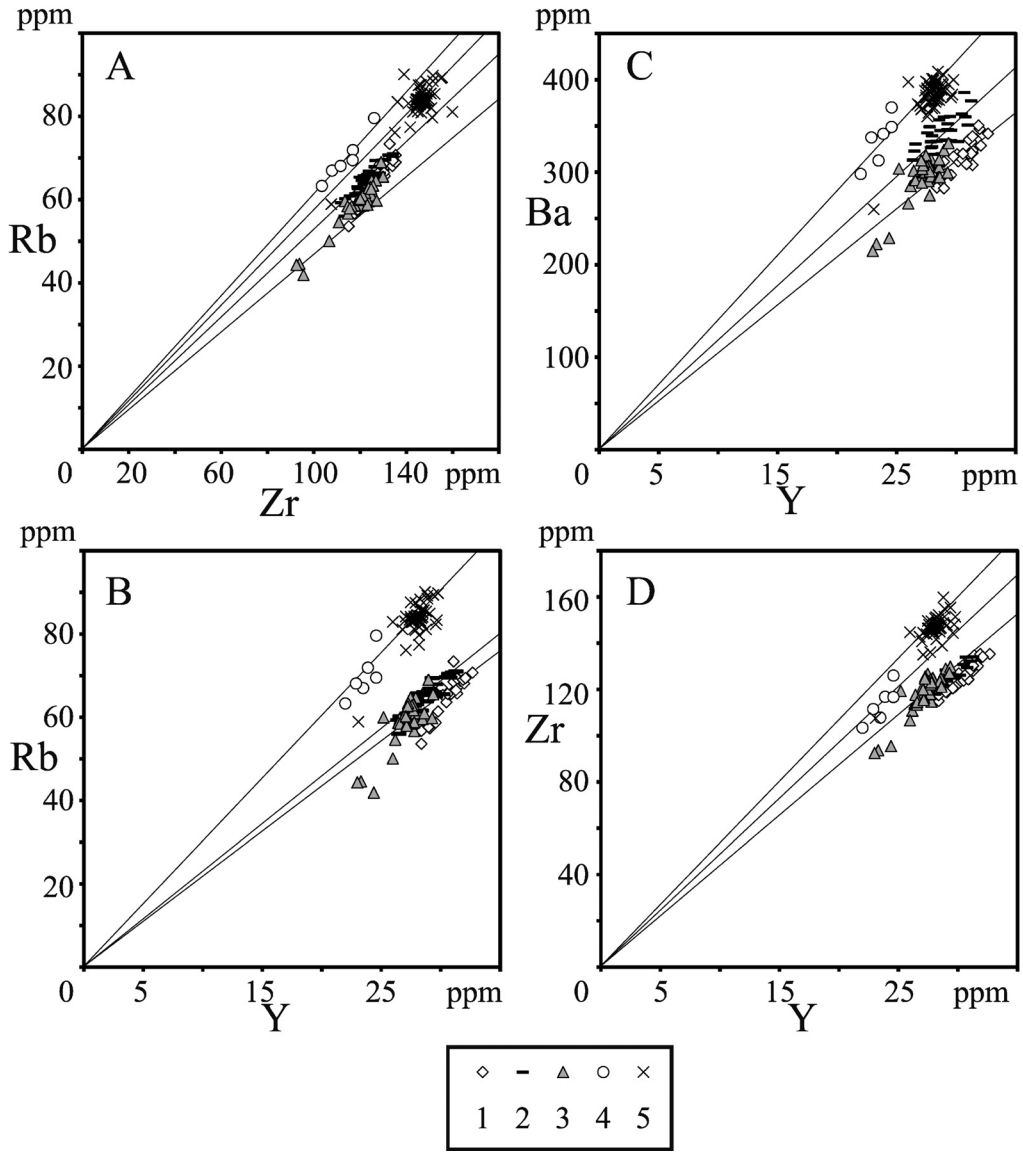


Fig. 14. Diagrams showing the incompatible trace element ratios of the lavas of boring core samples of drill-hole sites. A: Rb/Zr; B: Rb/Y; C: Ba/Y; D: Zr/Y. 1: An-ei subaqueous lava; 2: An-ei terrestrial lava; 3: Tenpyhoji lava; 4: younger Kitadake lava; 5: Harutayama lava.

Sakurajima volcano. The compositional trends of the low and high Ti-P types cannot be explained by magma mixing between the rhyolitic magma producing the pumice of the Iwato pyroclastic flow, Osumi pumice fall and Ito pyroclastic flow deposits and the basaltic andesitic magma yielded the MMI of the younger Kitadake lava, or by crystallization differentiation of the basaltic to basaltic andesitic magma produced the MMI of the younger Kitadake lava. This is consistent with the inference from the incompatible trace element ratios such as Rb/Zr, Rb/Y,

Ba/Y and Zr/Y.

The $^{87}\text{Sr}/^{86}\text{Sr}$ isotopic ratios of the felsic magma of the Sakurajima volcano and Aira caldera region since 61 ka are variable. The $^{87}\text{Sr}/^{86}\text{Sr}$ isotopic ratio of the high-silica rhyolitic magmas of the Osumi pumice fall and Ito pyroclastic flow deposit are 0.7058 to 0.7076, while those of the low Ti-P type dacitic magma (0.7054 to 0.7057) are higher than those of the high Ti-P type dacitic magma (0.7052 to 0.7054) (Kurasawa *et al.*, 1984; Arakawa *et al.*, 1998; Uto *et al.*, 2005). The $^{87}\text{Sr}/^{86}\text{Sr}$ isotopic ratios also

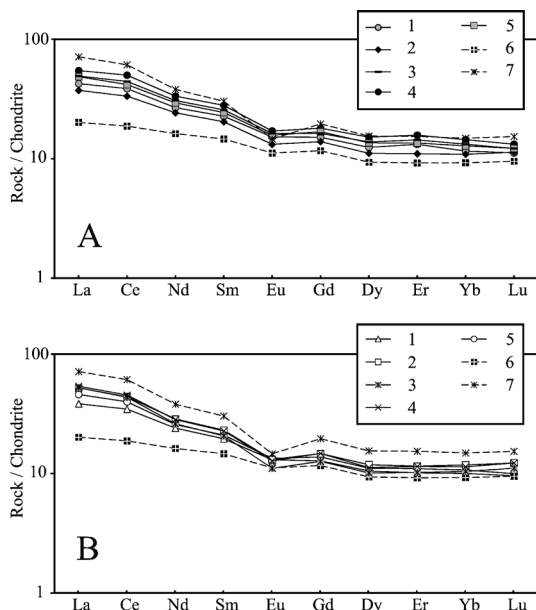


Fig. 15. Chondrite-normalized compositional pattern of rare earth elements for the eruptive products of the Sakurajima volcano. A: high Ti-P types; 1: Showa lava; 2: Taisho lava; 3: An-ei terrestrial lava; 4: Bunmei lava; 5: younger Minamidake lava; 6: mafic magmatic inclusion of the younger Kitadake lava; 7: Moeshima pumice; B: low Ti-P types; 1: older Minamidake lava; 2: Furihatayama-Harutayama lava; 3: Gongenyama lava; 4: Hikinohira lava; 5: younger Kitadake lava; 6: mafic magmatic inclusion of younger Kitadake lava; 7: Moeshima pumice.

support the conclusion that the felsic magmas consist of various types with different origin. On the view point of the $^{87}\text{Sr}/^{86}\text{Sr}$ isotopic ratios, the rhyolitic to high-silica rhyolitic magmas with relatively high $^{87}\text{Sr}/^{86}\text{Sr}$ isotopic ratios are considered to be the crustal origin (Arakawa *et al.*, 1998; Uto *et al.*, 2005).

The combination of magma mixing and crystallization differentiation is another alternative explanation. The crystallization differentiation of the mixed andesitic magma with various mixing ratios will give rise to the evolved felsic magmas with variable incompatible trace element ratios such as Rb/Y (Fig. 20); the andesitic magma was produced by magma mixing between the rhyolitic magma of the Iwato pyroclastic flow deposit or the high-silica rhyolitic magma of the Osumi pumice fall and Ito pyroclastic flow deposits, and the basaltic to basaltic andesitic magma yielding the magmatic inclusions of the Shikine andesite and the younger Kitadake lava of the Sakurajima volcano (Fig. 20). The felsic magma with higher Rb/Y ratio (the low Ti-P types) may have been

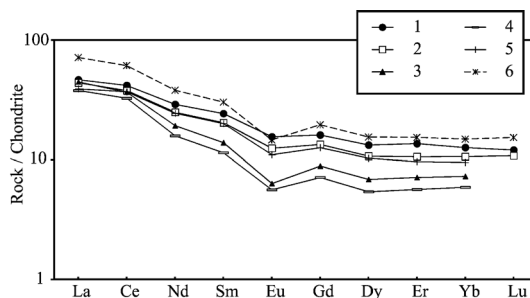


Fig. 16. Chondrite-normalized compositional pattern of rare earth elements for the eruptive products of the Aira caldera region. 1: average of high Ti-P types of the Sakurajima volcano; 2: average of low Ti-P types of the Sakurajima volcano; 3: average of the Ito pyroclastic flow deposit; 4: average of pumice of the Iwato pyroclastic flow deposit; 5: average of scoria of the Iwato pyroclastic flow deposit; 6: Moeshima pumice.

Table 1. The contents of rare earth elements of eruptive products of the Sakurajima volcano and Aira caldera region (in ppm). 1: Showa lava; 2: Taisho lava; 3: An-ei terrestrial lava; 4: Bunmei lava; 5: younger Minamidake lava; 6: older Minamidake lava; 7: younger Kitadake lava; 8: basaltic andesitic magmatic inclusion of the younger Kitadake lava; 9: Hikinohira lava; 10: Furihatayama lava; 11: Gongenyama lava; 12: Moeshima pumice; 13*: average of the Osumi air-fall pumice; 14*: average of pumice of the Ito pyroclastic flow deposit; 15*: average of pumice of the Iwato pyroclastic flow deposit; 16*: average of scoria of the Iwato pyroclastic flow deposit.

No	La	Ce	Nd	Sm	Eu	Gd	Dy	Er	Yb	Lu
1	16.07	37.71	19.16	5.21	1.32	4.70	4.85	3.37	2.89	0.43
2	14.11	32.59	17.35	4.68	1.14	4.32	4.33	2.80	2.71	0.44
3	18.61	43.30	21.97	5.90	1.41	5.07	5.38	3.66	3.29	0.47
4	20.65	48.89	23.94	6.44	1.48	5.60	5.91	4.02	3.60	0.51
5	18.38	40.75	21.01	5.60	1.36	5.24	5.29	3.45	3.19	0.47
6	14.52	33.77	17.18	4.50	1.13	3.96	4.10	2.58	2.50	0.37
7	17.36	38.94	18.41	4.82	1.16	4.29	4.32	2.80	2.66	0.39
8	7.62	18.30	11.61	3.37	0.97	3.62	3.65	2.35	2.30	0.37
9	19.70	42.82	20.49	5.31	1.13	4.56	4.62	2.94	2.94	0.47
10	20.35	44.31	20.26	5.22	1.10	4.58	4.37	2.92	2.83	0.47
11	19.78	42.45	18.65	4.76	0.96	3.93	3.94	2.60	2.59	0.43
12	26.97	59.74	27.21	6.96	1.27	6.08	6.03	3.91	3.70	0.59
13*	16.83	35.67	13.72	3.18	0.55	2.75	2.67	1.82	1.81	-
14*	17.52	36.26	14.31	3.32	0.56	2.93	2.78	1.84	1.87	-
15*	14.29	31.73	11.31	2.62	0.49	2.21	2.10	1.44	1.47	-
16*	14.74	35.95	17.44	4.59	0.95	3.91	4.00	2.45	2.36	-

derived from the mixed andesitic magma enriched in the felsic end-member component, while that with lower Rb/Y ratio (the high Ti-P types) is from the mixed andesitic magma depleted in the felsic end-member component (Fig.

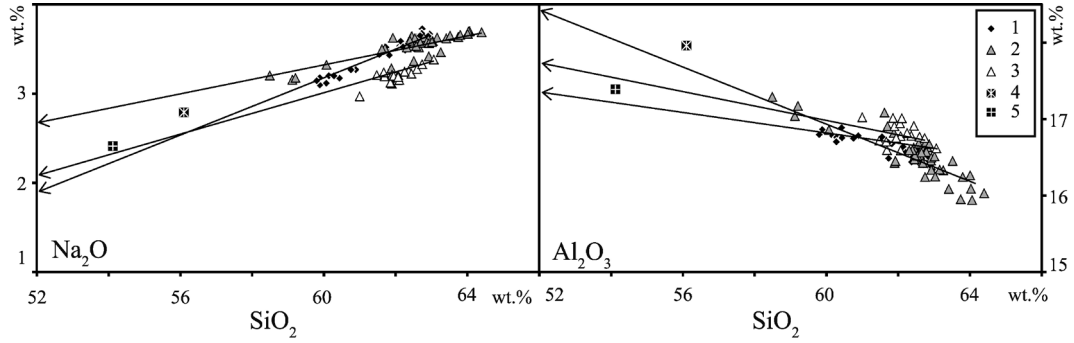


Fig. 17. Silica variation diagrams for Na₂O and Al₂O₃ contents of andesites of the Sakurajima volcano and Aira caldera region produced by the magma mixing. 1: Taisho lavas of the Sakurajima volcano; 2: Tenpyo-hoji (Nagasaki-bana) lavas of the Sakurajima volcano; 3: older Minamidake lavas of the Sakurajima volcano; 4: MMI in the younger Kitadake lava of Sakurajima volcano; 5: MMI in the Shikine andesite.

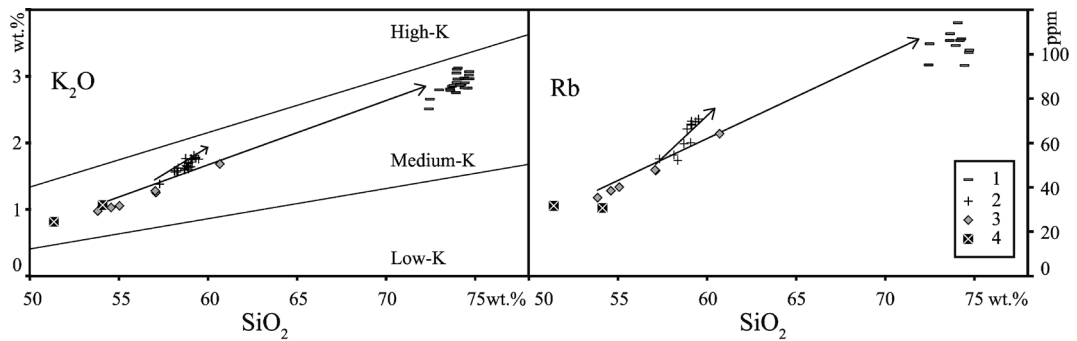


Fig. 18. Silica variation diagrams for K₂O and Rb contents of the Shikine andesite, andesitic scoria and rhyolitic pumice of the Iwato pyroclastic flow deposit. 1: pumice of the Iwato pyroclastic flow deposit; 2: scoria of the Iwato pyroclastic flow deposit; 3: Shikine andesite; 4: MMI in the Shikine andesite.

20).

The high Ti-P type felsic magma is higher in TiO₂, P₂O₅, Na₂O and FeO*, and lower in MgO and CaO, compared with the low Ti-P type felsic magma. It may be explained by assuming that the mafic end-member magma of the original mixed andesitic magma of the high Ti-P type is more differentiated and enriched in TiO₂, P₂O₅, Na₂O and FeO*, and depleted in MgO and CaO, while that of the low Ti-P types is less differentiated and depleted in TiO₂, P₂O₅, Na₂O and FeO*, and enriched in MgO and CaO (Fig. 21). On the other hand, the original mixed andesitic magma of the low Ti-P types is more enriched in the felsic end-member component than that of the high Ti-P types, because the Rb/Y ratio of the low Ti-P types is higher than that of the high Ti-P types (Fig. 20).

The ⁸⁷Sr/⁸⁶Sr isotopic ratios of the felsic end-member magma is high (0.7058 to 0.7076), while that of the basaltic andesitic MMI of the younger Kitadake lava, which is one of the plausible candidates for the mafic end-

member magma, is low (0.7050) (Kurasawa *et al.*, 1984; Arakawa *et al.*, 1998; Uto *et al.*, 2005). The ⁸⁷Sr/⁸⁶Sr isotopic ratios of the high Ti-P type felsic magma (0.7052 to 0.7054) are lower than those of the low Ti-P type felsic magma (0.7054 to 0.7057) (Kurasawa *et al.*, 1984; Arakawa *et al.*, 1998; Uto *et al.*, 2005). The lower ⁸⁷Sr/⁸⁶Sr isotopic ratios of the high Ti-P type felsic magmas imply that their original magmas are enriched in the mafic end-member component with low ⁸⁷Sr/⁸⁶Sr isotopic ratios.

Kay *et al.* (2010) proposed the La/Sm vs. Sm/Yb discrimination diagram to distinguish the constituent minerals of the source rocks of the felsic magmas. The La/Sm ratio means the degree of enrichment of incompatible element in the source rocks, while the Sm/Yb ratio indicates the source rock mineralogy reflecting the pressure. As the Sm/Yb ratio increases, the constituent mafic minerals of the source rocks change from pyroxene, hornblende to garnet, which indicate the increase of pressure. The source rock mineralogy of the rhyolitic to high-silica

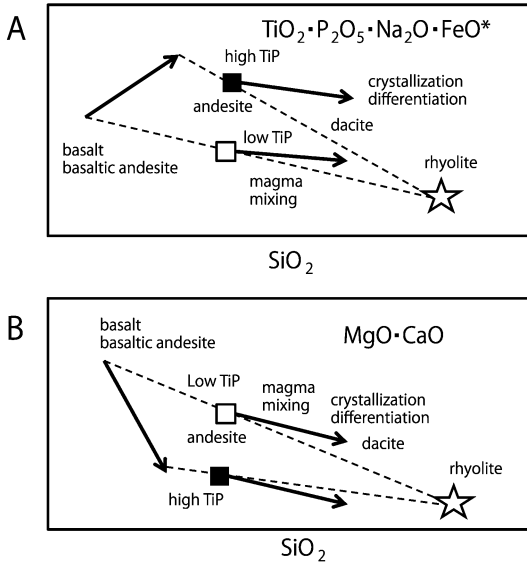


Fig. 21. Schematic silica variation diagram showing the genetic process of dacitic magmas produced by the crystallization differentiation of andesitic magma formed by the magma mixing between the basaltic to basaltic andesitic magma and the rhyolitic to high-silica rhyolitic magma. Arrows indicate the trend of crystallization differentiation and solid lines show the magma mixing line. A: TiO_2 , P_2O_5 , Na_2O and FeO^* contents; B: MgO and CaO contents; star: felsic end-member magma (rhyolite); solid square: high Ti-P type andesitic magma; open square: low Ti-P type andesitic magma.

produced by the crystallization differentiation of mixed andesitic magmas, the high Ti-P type mixed andesitic magma is enriched in the component of high temperature mafic end-member magma. The core compositions of orthopyroxene phenocryst of the low Ti-P types are more magnesian than those of the high Ti-P types (Fig. 24), suggesting that the mafic end-member magma of the low Ti-P types was less evolved and the mixed magma was more magnesian, which probably caused the relatively magnesian nature of the dacitic magma of the low Ti-P types (Fig. 24).

The two different explanations for the chemical variations of the eruptive products of the Sakurajima volcano and Aira caldera region since 61 ka are briefly summarized and schematically shown in Fig. 25.

7-4 Evolution of the magma chamber system of the Sakurajima volcano and Aira caldera region since 61 ka

The evolution of the magma chamber system of the Sakurajima volcano and Aira caldera region since 61 ka is summarized in Fig. 4.

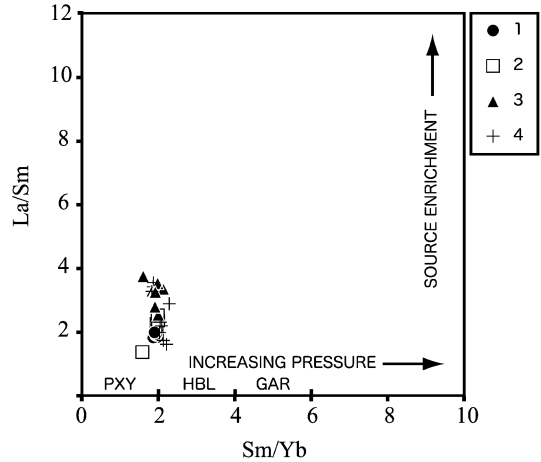


Fig. 22. La/Sm vs. Sm/Yb diagram by Kay *et al.* (2010). The La/Sm ratio shows the degree of source enrichment and the Sm/Yb ratio indicates the source rock mineralogy. The Sm/Yb ratios of the felsic eruptive products of the Sakurajima volcano and Aira caldera region suggest that their source rocks are pyroxene bearing. 1: low Ti-P types; 2: high Ti-P types; 3: Osumi pumice fall and Ito pyroclastic flow deposits; 4: Iwato pyroclastic flow deposit; PXY: pyroxene bearing; HBL: hornblende bearing; GAR: garnet bearing.

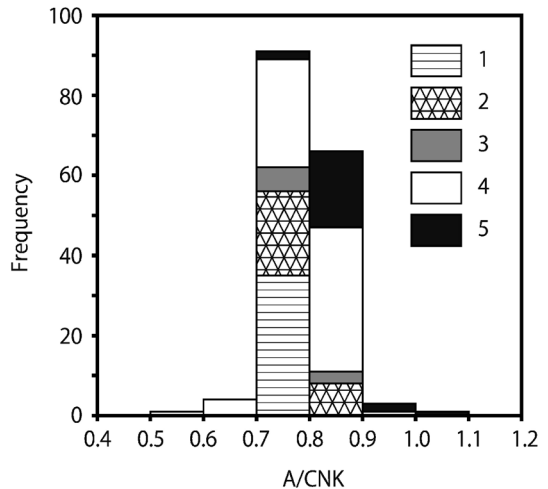


Fig. 23. Histogram showing the $\text{Al}_2\text{O}_3/(\text{CaO} + \text{Na}_2\text{O} + \text{K}_2\text{O})$ ratios. The $\text{Al}_2\text{O}_3/(\text{CaO} + \text{Na}_2\text{O} + \text{K}_2\text{O})$ molar ratios of felsic eruptive products ($> 63\% \text{SiO}_2$) are mostly less than 1.1 and metaluminous, showing that their source rocks are not pelitic but igneous in composition. 1: high Ti-P types; 2: low Ti-P types; 3: Moeshima pumice; 4: Osumi pumice fall and Ito pyroclastic flow deposits; 5: Iwato pyroclastic flow deposit (pumice).

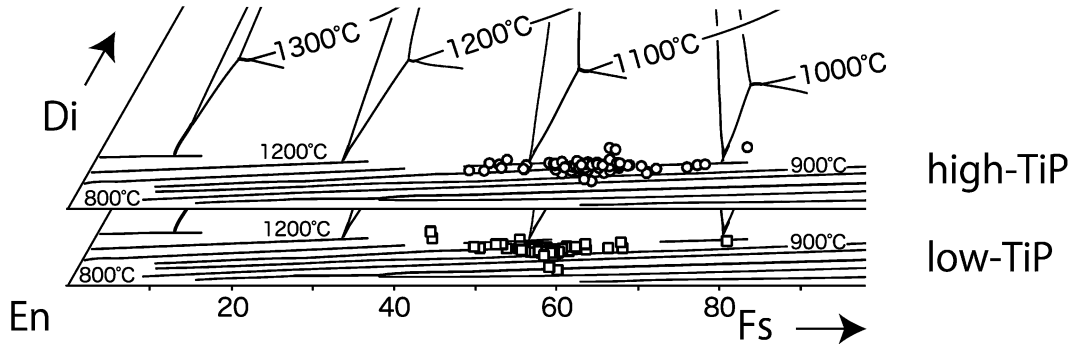


Fig. 24. The estimation of temperature of the high Ti-P and low Ti-P type magmas by the pyroxene geothermometer of Lindsley (1981) at 5 kb. The core compositions of phenocrystic orthopyroxenes coexisting with phenocrystic clinopyroxenes are presented. The numerals indicate the temperature in $^{\circ}\text{C}$. The temperature of the high Ti-P types estimated from the core composition of phenocrystic orthopyroxenes is higher than that of the low Ti-P types. The estimated temperatures of the high Ti-P types are 1000°C to 1100°C and those of the low Ti-P types are 900°C to 1000°C , respectively. Di: diopside; En: enstatite; Fs: ferrosilite.

Around 61 to 60 ka, the andesitic magma chamber system was active beneath the Aira caldera region, and the Shikine andesite lavas (53 to 60 wt%SiO₂) and the scoria of the Iwato pyroclastic flow deposit (57 to 59 wt%SiO₂) were erupted. Concurrently, the large-scale felsic magma chamber was formed, which produced the pumice of the Iwato pyroclastic flow deposit (72 to 74 wt%SiO₂) with a volume of exceeding 20 km³.

Most andesitic magma in this stage was thought to be formed by magma mixing between the basaltic to basaltic andesitic magmas of mantle origin and the felsic magmas of crustal origin, some of which yielding the pumice of the Iwato pyroclastic flow deposit.

Bachman and Bergantz (2008) classified the style of magma chambers, which gives rise to the large-scale eruption of voluminous felsic magma, into the three groups. The Group 1 comprises the upper crystal-poor rhyolitic magma grading to the lower crystal-rich less differentiated felsic magma. The Group 2 consists of the felsic magma having almost no compositional gradient. The Group 2 is further subdivided into (a) the crystal-poor rhyolitic magma and (b) the crystal-rich dacitic magma. The Group 3 is composed of the upper crystal-poor rhyolitic magma shift abruptly to the lower crystal-rich less differentiated magma.

The magma chamber of the Iwato pyroclastic flow deposit probably belongs to the Group 3; the rhyolitic pumice with phenocryst content of about 10vol.% was derived from the upper crystal-poor rhyolitic portion and the andesitic scoria with phenocryst content of about 30vol.% originated from the lower crystal-rich andesitic part of the magma chamber, though both magmas had no genetic relations in chemistry. Otherwise, the magma chamber of the Iwato rhyolitic pumice was independent

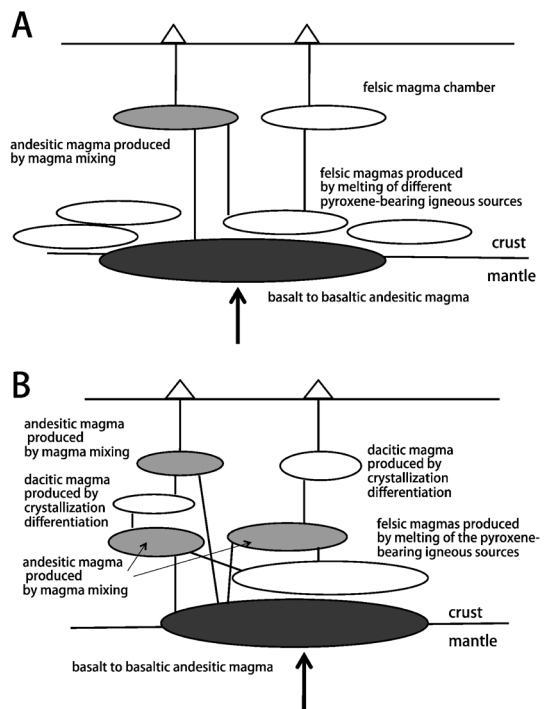


Fig. 25. Schematic diagram showing the mode of magma generation in the Sakurajima volcano and Aira caldera region. A: explanation in which felsic magmas (including dacitic magma) were formed by melting of the different source rocks (the case for both the Sakurajima volcano and Aira caldera region); B: explanation in which dacites were produced by the crystallization differentiation of mixed andesitic magma (the case for the Sakurajima volcano).

from that of the Iwato andesitic scoria; the eruption of the Iwato rhyolitic pumice triggered the eruption of other magma chamber filled with the andesitic magma of the Iwato scoria.

After a long dormant period of about twenty-four thousands of years, the felsic volcanic activity resumed at 36 ka in the Aira caldera region. The climactic gigantic eruption at 29 ka with a volume of 450 km³ produced the pumice and ash of high-silica rhyolite (74 to 76 wt. %SiO₂), the magma chamber of which is nearly uniform and monotonous in composition and classified as the Group 2(a) of Bachman and Bergantz (2008). The low temperature high-silica rhyolitic magma of the Osumi pumice fall and Ito pyroclastic flow deposits can be derived from the rhyolitic magma erupted as the Iwato pyroclastic flow deposit by crystallization differentiation. Both felsic magmas are similar in composition and probably comprise the same magma chamber system. The rhyolitic magma chamber system which produced the Iwato pyroclastic flow, Osumi pumice fall and Ito pyroclastic flow deposits was long-lived, the duration of which was as long as thirty thousands of years. The long duration probably resulted in the storing of voluminous felsic magma and the formation of gigantic-scale felsic magma chamber beneath the Aira caldera region at the time of the climactic eruption. It was difficult for basaltic to basaltic andesitic magmas to penetrate the gigantic felsic magma chamber, causing the lack of basaltic to andesitic volcanic activity in the Aira caldera region at this period, except for the southern margin of the Aira caldera where small amount of andesitic lavas erupted. The magma chamber system of the voluminous high-silica rhyolite was destroyed completely by the large catastrophic eruption at 29 ka.

After a quiescent period of about three thousands of years, the volcanic activity resumed and the magma chamber system of the Sakurajima volcano began to feed the dacitic to andesitic magmas to the surface.

The magma chamber system of the Sakurajima volcano is not simple on the view point of the whole-rock chemistry; it is composed of the low and high Ti-P type dacitic magmas. During the period from 26 to 13 ka, the magma chamber systems of the rhyolite (the Moeshima rhyolite) and dacite coexisted beneath the Sakurajima volcano and Aira caldera region. The magma chamber system of the Moeshima rhyolite was probably independent from that of the Sakurajima volcano. The magma chamber systems with the relatively low temperature low Ti-P type dacitic magma were active during the period from 13 to 4 ka beneath the Sakurajima volcano and Aira caldera region, which further comprised at least more than three different sub-systems based on the whole-rock chemistry of felsic volcanic rocks; they are represented by the Gongenyama, Furihatayama-Harutayama, and younger Kitadake-Hikinohira dacitic lava groups. The andesite

formed by the magma mixing was not dominant during this period. The low Ti-P type older Minamidake andesite lavas are akin to the lavas of the younger Kitadake stage in chemical composition; they belong to either the last stage of the Kitadake volcano or the earliest member of the Minamidake volcano.

The magma chamber system of the historical eruptions with the relatively high temperature high Ti-P type dacitic magma consists of the three sub-systems; they are represented by the Tenpyohoji, younger Minamidake-Bunmei-An-ei terrestrial, and An-ei subaqueous lava groups mainly on the basis of the whole-rock chemistry. Among them, both the Tenpyohoji and An-ei subaqueous magma chamber sub-systems erupted andesitic magma produced by magma mixing; they are the Nagasakibana, Taisho and Showa lavas.

The each magma chamber sub-system of the Sakurajima volcano is short-lived with duration of thousands to several hundreds of years. The onset of the magma chamber sub-system of the present volcanic activity of the Sakurajima volcano was probably the An-ei subaqueous eruption at 1779AD.

8. Summary and conclusion

(1) The eruptive products of the Sakurajima volcano consist of the high Ti-P and low Ti-P type dacite to andesite. The high Ti-P types are enriched in Na₂O, FeO*, Zr, Nb and Y, and depleted in MgO, Al₂O₃ and CaO, compared with the low Ti-P types. The incompatible trace element ratios, such as Rb/Y, Rb/Zr, Ba/Y and Zr/Y, of the high Ti-P types are lower than those of the low Ti-P types. The LREE/HREE ratios such as La/Yb are lower in the high Ti-P types. The ⁸⁷Sr/⁸⁶Sr isotopic ratios of the high Ti-P types (0.7051 to 0.7054) are lower than those of the low Ti-P types (0.7055 to 0.7057). It is difficult to derive both types from the same parental mafic magma by simple crystallization differentiation.

(2) The high Ti-P and low Ti-P types of the Sakurajima volcano are classified into at least the six sub-groups based on the whole-rock chemical compositions, especially major element chemistry. The high Ti-P types are composed of the three sub-groups: the Tenpyohoji, the younger Minamidake-Bunmei-An-ei terrestrial, and the An-ei subaqueous-Taisho-Showa lava groups, while the low Ti-P types consist of the three sub-groups: the Gongenyama, the Furihatayama-Harutayama, and the younger Kitadake - Hikinohira lava groups.

(3) The Moeshima rhyolitic pumice erupted in the Aira caldera is lower in TiO₂, P₂O₅, MgO, Al₂O₃ and CaO, and higher in Na₂O, K₂O, FeO* and MnO than those of the Iwato pyroclastic flow, Osumi pumice fall and Ito pyroclastic flow deposits. The incompatible trace element ratios, such as Rb/Y, Rb/Zr, Ba/Y and Zr/Y, of the Moeshima rhyolite are lower than those of the Iwato pyroclastic flow, Osumi pumice fall and Ito pyroclastic

flow deposits. The Moeshima pumice is more enriched in REE content and lower in LREE/HREE ratios, such as La/Yb, than the Iwato pyroclastic flow, Osumi pumice fall and Ito pyroclastic flow deposits.

(4) The high-silica rhyolitic magma producing the Osumi pumice fall and Ito pyroclastic flow deposits can be derived from the rhyolitic magma of the Iwato pyroclastic flow deposit by crystallization differentiation.

(5) The mafic volcanic rocks are present as lavas in the Shikine andesite and as MMIs of the Shikine andesite and the Kitadake lava of the Sakurajima volcano. They are medium-K basalt to basaltic andesite. The basaltic andesite of the Shikine andesite can be produced by the crystallization differentiation of basalt of the Shikine andesite. The basaltic magma continued to ascend constantly from the mantle to the crust and probably to supply enough heat to the lower crust to produce felsic magmas since 61 ka.

(6) The andesite of the Sakurajima volcano and Aira caldera region are the products of magma mixing. The magma mixing between the magma of the Shikine andesite and felsic end-member magma more enriched in K_2O and Rb than the rhyolitic magma of the Iwato pyroclastic flow deposit gave rise to the andesitic scoria of the Iwato pyroclastic flow deposit. The low Ti-P type andesites of the Sakurajima volcano were produced by magma mixing between the basaltic to basaltic andesitic magma giving rise to the MMI of the younger Kitadake lava and the low Ti-P type dacitic magma, while the high Ti-P type andesites can be produced by magma mixing between the basaltic to basaltic andesitic magma being akin to the MMI of the younger Kitadake lava and the high Ti-P type dacitic magma.

(7) The felsic magmas of the Sakurajima volcano and Aira caldera region consist of at least eight different types. They may be generated independently by the melting of pyroxene-bearing crustal source rocks with different compositions. The alternative explanation is that they were derived from the andesitic magma with various mixing ratios by crystallization differentiation, the end-member magmas of which were the basaltic to basaltic andesitic magma and the rhyolitic to high-silica rhyolitic magma of the Iwato pyroclastic flow, Osumi pumice fall and Ito pyroclastic flow deposits. The low Ti-P type dacitic magma of the Sakurajima volcano is derived from the andesitic magma by crystallization differentiation, which is produced by magma mixing between the less differentiated basaltic magma and the rhyolitic to high-silica rhyolitic magma; the low Ti-P type mixed andesitic magma is more enriched in the felsic end-member component. Contrarily, the high Ti-P type dacite is derived from the andesitic magma by crystallization differentiation, which is formed by magma mixing between the evolved basaltic to basaltic andesitic magma and the rhyolitic to high-silica rhyolitic magma; the high Ti-P type mixed andesitic magma is more depleted in the felsic end-

member component.

(8) In the Aira caldera region, the andesite magma chamber system was active around 61 ka, in which the magma mixing between basaltic magma and rhyolitic magma was taken place, feeding the Shikine andesite lava to the surface. In 60 ka, the relatively large-scale magma chamber system of the rhyolite was developed, which was accompanied by the andesitic magma produced by magma mixing, erupting the pumice and scoria of the Iwato pyroclastic flow deposit. The size of the rhyolitic magma chamber increased during a quiescent period of twenty-four thousands of years, constructing a gigantic magma chamber filled with voluminous high-silica rhyolitic magmas, resulted in the catastrophic eruption which formed the Osumi pumice fall, Ito pyroclastic flow, and AT ash fall deposits. During the period from 35 ka to 29 ka, no andesite erupted in the Aira caldera region; it is because the basaltic to basaltic andesitic magma could not penetrate the gigantic felsic magma chamber beneath the Aira caldera and could not reach the surface. The magma chamber system of the rhyolitic to high-silica rhyolitic magma was long-lived and maintained for as long as thirty thousands of years.

After a dormant period of three thousands of years, the small to intermediate-scale magma chamber system comprising dacitic magma started to feed magmas to the surface. The supply of basaltic to basaltic andesitic magma to the dacitic magma chamber produced the mixed andesitic magma. At 13.8 ka, the subaqueous eruption of the Moeshima rhyolitic magma occurred in the Aira caldera, which was not directly related to the volcanic activity of the Sakurajima volcano and probably comprised the independent magma chamber system. The low Ti-P type magma chamber system was active during 13.8 ka to 4 ka in the Sakurajima volcano, which consists of at least three sub-systems. The high Ti-P type magma chamber system was dominant since the historical Tenpyohoji eruption at 8th C and continued until now, which comprised three sub-systems. The onset of the youngest sub-system is the An-ei subaqueous eruption at 1779AD. The duration of the activity of each magma chamber sub-systems of the Sakurajima volcano is rather short, which is thousands to hundreds of years.

Acknowledgement

We are grateful for Profs. Tagiri, M. and Fujinawa, A. of the Ibaraki University for their discussions and help of chemical analysis by XRF and ICP apparatus. We also thank Shimada, J., Atsuchi, T., Umezawa, T., Shiroishi, T., Ichiki, Y., and Satake, S., the undergraduate students of the Department of Geosystem Sciences of the Nihon University, for their assistance of sampling and chemical analysis. We appreciate Prof. Nakada, S. of the Earthquake Research Institute of University of Tokyo for permitting the use of XRF apparatus. We thank the Sakurajima Vol-

cano Research Center of Disaster Prevention Research Institute of Kyoto University for providing the boring core samples of drill-hole sites and permitting us to use them for the chemical analysis. We also appreciate the review and helpful advices of Prof. Nakamura, M. of the Tohoku University and another anonymous reviewer, which was useful for improving the manuscript.

References

- Arakawa, Y., Kurosawa, M., Takahashi, K., Kobayashi, Y., Tsukui, M. and Amakawa, H. (1998) Sr-Nd isotopic and chemical characteristics of the silicic magma reservoir of the Aira pyroclastic eruption, southern Kyushu, Japan. *J. Volcanol. Geotherm. Res.*, **80**, 179–194.
- Aramaki, S. (1971) Hydrothermal determination of temperature and water pressure on the magma of Aira caldera. *Am. Mineral.*, **56**, 1760–1768.
- Aramaki, S. (1984) Formation of Aira caldera, southern Kyushu. *J. Geophys. Res.*, **89**, 8485–8501.
- Bachman, O. and Bergantz, G. (2008) The magma reservoirs that feed supereruptions. *Elements*, **4**, 29–34.
- Fukushima, D. and Kobayashi, T. (2000) Mechanism of generation and emplacement of the Tarumizu pyroclastic flow associated with Osumi plinian eruption from Aira caldera, Japan. *J. Volcanol. Soc. Japan*, **45**, 225–240 (in Japanese).
- Hiyadati, S., Ishihara, K. and Iguchi, M. (2007) Volcano-tectonic earthquakes during the stage of magma accumulation at the Aira caldera, southern Kyushu, Japan. *J. Volcanol. Soc. Japan*, **52**, 289–310.
- Iguchi, M. (2007) Aira caldera storing magma. *Chikyū Monthly*, **28**, 116–122 (in Japanese).
- Kano, K., Yamamoto, T. and Ono, K. (1996) Subaqueous eruption and emplacement of the Shinjima pumice, Shinjima (Moeshima) island, Kagoshima bay, SW Japan. *J. Volcanol. Geotherm. Res.*, **71**, 187–206.
- Kay, S.M., Coira, B.L., Caffè, P.J. and Chen, C.H. (2010) Regional chemical diversity, crustal and mantle sources and evolution of central Andean Puna plateau ignimbrites. *J. Volcanol. Geotherm. Res.*, **198**, 81–111.
- Kobayashi, T. (2009) Origin of new islets (An-ei islets) formed during the An-ei eruption (1779–1782) of Sakurajima volcano, southern Kyushu, Japan. *J. Volcanol. Soc. Japan*, **54**, 1–13 (in Japanese).
- Kobayashi, T. (2010) Geology of Sakurajima volcano: unsolved issues. *Abstracts, the 117th Annual Meeting of the Geological Society of Japan*. p123 (in Japanese).
- Kobayashi, T. and Ezaki, K. (1997) Sakurajima volcano, reexamination of its history of eruption. *Chikyū Monthly*, **19**, 227–231 (in Japanese).
- Kurasawa, H., Arai, F. and Machida, H. (1984) Strontium isotopic identification of the widespread Aira-Tn ash-fall deposits (AT) in Japan. *J. Volcanol. Soc. Japan.*, **29**, 115–118 (in Japanese).
- Lindsley, D.H. (1983) Pyroxene thermometry. *Am. Mineral.*, **68**, 477–493.
- Machida, H. and Arai, F. (2003) Atlas of tephra in and around Japan. revised edition. Tokyo Univ. Press. 336p (in Japanese).
- Miki, D. (1999) Estimation of the age of lava flows at Sakurajima volcano, Kyushu, Japan; inferred from paleomagnetic directions and paleointensities. *J. Volcanol. Soc. Japan*, **44**, 111–122 (in Japanese).
- Miki, D., Uto, K., Utsumi, S. and Ishihara, K. (2000) K-Ar dating and paleomagnetic measurements on drilled cores from the Sakurajima volcano: Part 2. *Annuals of Disas. Prev. Res. Inst., Kyoto Univ.*, **43B-1**, 1–6 (in Japanese).
- Miki, D., Uto, K., Sudo, M. and Ishihara, K. (2003) Correlation of lavas on drilled cores from the Sakurajima volcano, inferred from paleomagnetic and chemical features. *Annuals of Disas. Prev. Res. Inst., Kyoto Univ.*, **46B**, 835–840 (in Japanese).
- Moriwaki, H. (1992) Late Quaternary phreatomagmatic tephra layers and their relation to paleo-sea levels in the area of Aira caldera, southern Kyushu, Japan. *Quaternary International*, **13/14**, 195–200.
- Nagaoka, S. (1988) Late Quaternary tephra layers from the caldera volcanoes in and around Kagoshima bay, southern Kyushu, Japan. *Geogr. Rep. Tokyo Metropolitan Univ.*, **23**, 49–122.
- Nagaoka, S., Okuno, M. and Arai, F. (2001) Tephrostratigraphy and eruptive history of the Aira caldera volcano during 100–30 ka, Japan. *J. Geol. Soc. Japan*, **107**, 432–450 (in Japanese).
- Okuno, M. (1997) Radiocarbon dating of the Sakurajima tephra group. *Chikyū Monthly*, **19**, 231–235 (in Japanese).
- Okuno, M. (2002) Chronology of tephra layers in southern Kyushu, SW Japan, for the last 30,000 years. *Quaternary Res.*, **41**, 225–236 (in Japanese).
- Rollinson, H. (1993) Using geochemical data: evaluation, presentation, interpretation. Longman Singapore Publisher, 352p.
- Sudo, M., Ishihara, K. and Tatsumi, Y. (2000a) Pre-caldera volcanic history in Aira caldera area: K-Ar datings of lavas from Kajiki and Kokubu areas in northern part and Ushine area in southern part of the caldera. *J. Volcanol. Soc. Japan*, **45**, 1–12 (in Japanese).
- Sudo, M., Uto, K., Miki, D., Ishihara, K. and Tatsumi, Y. (2000b) K-Ar dating of volcanic rocks along the Aira caldera rim -Volcanic history before explosive Aira pyroclastic eruption-. *Annuals of Disas. Prev. Res. Inst., Kyoto Univ.*, **43B-1**, 15–35 (in Japanese).
- Sudo, M., Uto, K., Miki, D. and Ishihara, K. (2001) K-Ar dating of volcanic rocks along the Aira caldera rim: Part 2- Volcanic history of western and northwestern area of caldera and Sakurajima volcano-. *Annuals of Disas. Prev. Res. Inst., Kyoto Univ.*, **44B-1**, 305–316 (in Japanese).
- Tagiri, M. and Fujinawa, A. (1988) Chemical analysis of REE and trace metals in GSJ rock reference samples by ICP. *J. Min.Petr.Econ.Geol.*, **83**, 102–106 (in Japanese).
- Takahashi, M., Otsuka, T., Kawamata, H., Sako, H., Yasui, M., Kanamaru, T., Otsuki, M., Shimada, J., Atsuchi, T., Umezawa, T., Shiroishi, T., Ichiki, Y., Satake, S., Kobayashi, T., Ishihara, K. and Miki, D. (2011) Whole-rock chemistry for eruptive products of the Sakurajima

- volcano and Aira caldera, southern Kyushu: summary of 583 analytical data. *Proceedings Inst. Natur. Sci. Nihon Univ.*, **46**, 133-200 (in Japanese).
- Tatsumi, Y. and Inoue, H. (1993) Rhyolite from Okogashima island, Kagoshima Prefecture. K-Ar ages and petrological characteristics. *Annuals of Disas. Prev. Res. Inst. Kyoto Univ.*, **36B-1**, 231-236 (in Japanese).
- Tsukui, M. and Aramaki, S. (1990) The magma reservoir of the Aira pyroclastic eruption- A remarkably homogeneous high-silica rhyolite magma reservoir. *Bull. Volcanol. Soc. Jpn.*, **35**, 231-248 (in Japanese).
- Uto, K., Miki, D., Uchiumi, S. and Ishihara, K. (1999) K-Ar dating and paleomagnetic measurements on drilled cores from the Sakurajima volcano- Preliminary attempts to reveal the history of the volcanic activity. *Annuals of Disas. Prev. Res. Inst. Kyoto Univ.*, **42B-1**, 27-34 (in Japanese).
- Uto, K., Miki, D., Nguyen, H., Sudo, M., Fukushima, D. and Ishihara, K. (2005) Temporal evolution of magma composition in Sakurajima volcano, Southwest Japan. *Annuals of Disas. Prev. Res. Inst. Kyoto Univ.*, **48B**, 341-347 (in Japanese).
- Wallace, M., Ellis, S., Miyao, K., Miura, S. Beavan, J. and Goto, J. (2009) Enigmatic, highly active left-lateral shear zone in southwest Japan explained by aseismic ridge collision. *Geology*, **37**, 143-146.
- Yamaguchi, K. (1975) Sakurajima volcano: Geological and petrological study of the surrounding area of the Kagoshima bay and Sakurajima volcano. *Jap. Earth Sci. Educ. Soc. Tokyo*, 128p (in Japanese).
- Yanagi, T., Ichimaru, Y. and Hirahara, S. (1991) Petrochemical evidence for coupled magma chambers beneath the Sakurajima volcano, Kyushu, Japan. *Geochem. J.*, **25**, 17-30.
- Yasui, M., Takahashi, M., Ishihara, K. and Miki, D. (2007) Eruptive style and its temporal variation through the 1914-1915 eruption of Sakurajima Volcano, southern Kyushu, Japan. *Bull. Volcanol. Soc. Japan*, **52**, 161-186 (in Japanese).
- Yasui, M., Takahashi, M., Shimada, J., Ishihara, K. and Miki, D. (2013) Comparative study of proximal eruptive events in the large-scale eruptions of Sakurajima Volcano: the An-ei vs. Taisho eruption. submitted to *the special issue of Bull. Volcanol. Soc. Japan*. **58**, 59-76.

(Editorial handling Masao Ban)

桜島火山および始良カルデラ地域における 61 ka 以降のマグマ化学組成の 時間変化とマグマ溜りシステムの進化

高橋正樹・大塚 匡・迫 寿・川俣博史・安井真也・金丸龍夫・
大槻 明・小林哲夫・石原和弘・味喜大介

桜島火山および始良カルデラ地域における 61 ka 以降のマグマ化学組成の時間変化とマグマ溜りシステムの進化について噴出物の全岩化学組成に基づいて検討した。61 ka 以降の桜島火山および始良カルデラ地域のマグマは、(1) マントル起源の玄武岩質および玄武岩質安山岩質マグマ、(2) 地殻起源の流紋岩質および高シリカ流紋岩質マグマ、(3) デイサイト質マグマ、(4) マグマ混合によって形成された安山岩質マグマ、の 4 グループに分けられる。始良カルデラ地域では、61 ka 頃に玄武岩質、玄武岩質安山岩質、安山岩質そして流紋岩質マグマの活動があり、敷根安山岩や安山岩質スコリアおよび流紋岩質軽石からなる岩戸火砕流堆積物が噴出した。24,000 年ほどの静穏期の後に流紋岩質マグマの活動が再開し、29 ka には大量の高シリカ流紋岩質マグマが噴出して、大隅降下軽石堆積物および入戸火砕流堆積物が形成された。60 ka の岩戸火砕流堆積物の流紋岩質マグマと、29 ka の大隅降下軽石堆積物および入戸火砕流堆積物の高シリカ流紋岩質マグマは同源と考えられ、前者の結晶分化作用によって後者が形成されたと考えられる。始良カルデラ地域では 30,000 年余りの期間にわたって、流紋岩質～高シリカ流紋岩質からなるマグマ溜りが長期に安定であったものと推定される。3,000 年余りの静穏期の後、桜島火山の活動が 26 ka に開始された。13.8 ka には始良カルデラ内で燃島軽石の海底噴火が生じたが、これは桜島火山とは別のマグマ溜りシステムからもたらされたものと考えられる。桜島火山のマグマ溜りシステムは、高 Ti-P タイプおよび低 Ti-P タイプのデイサイト質および安山岩質マグマからなる。このうちの安山岩質マグマは、玄武岩質～玄武岩質安山岩質マグマと高 Ti-P タイプおよび低 Ti-P タイプのデイサイト質マグマのマグマ混合によって形成された。低 Ti-P タイプのマグマ溜りシステムは 14 ka から 4 ka に活動的であり、全岩化学組成からは少なくとも 3 つのサブシステムからなる。8 世紀以降の歴史時代噴出物は高 Ti-P タイプであり、全岩化学組成からは 3 つのサブシステムからなるが、最新のものは 1779 年 AD の安永海底噴火以降に噴出したものである。桜島火山のそれぞれのマグマ溜りシステムの持続時間は数 100 年から数 1,000 年程度と短い。